ISSN: 1863-5598

ZKZ 64717
08-21

Bodo´s Power Systems®

Electronics in Motion and Conversion

August 2021

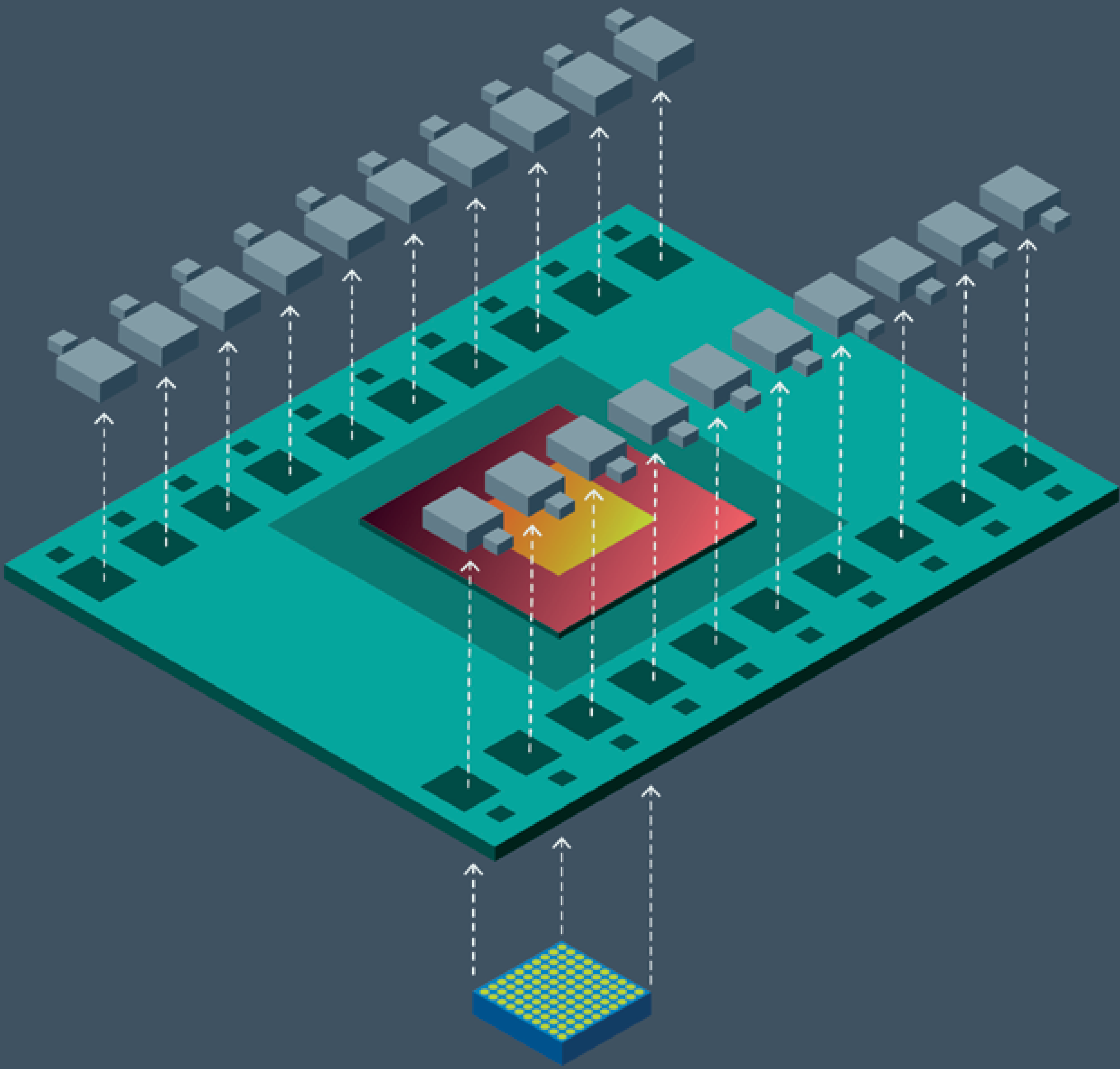

Transforming power delivery
for high-performance processors

VICOR

PULSED INDUCTANCE MEASUREMENT

POWER CHOKE TESTER DPG10/20 SERIES

Inductance measurement from 0.1 A to 10 kA

KEY FEATURES

Measurement of the

- **Incremental inductance** $L_{inc}(i)$ and $L_{inc}(\int Udt)$
- **Secant inductance** $L_{sec}(i)$ and $L_{sec}(\int Udt)$
- **Flux linkage** $\psi(i)$
- **Magnetic co-energy** $W_{co}(i)$
- **Flux density** $B(i)$
- **DC resistance**

Also suitable for 3-phase inductors

WIDE RANGE OF MODELS

7 models available with maximum test current from 100A to 10000A and maximum pulse energy from 1350J to 15000J

KEY BENEFITS

- Very **easy and fast** measurement
- **Lightweight, small and affordable price-point** despite of the high measuring current up to 10000A
- **High sample rate and very wide pulse width range** => suitable for all core materials

APPLICATIONS

Suitable for all inductive components from **small SMD inductors** to **very large power reactors in the MVA range**

- **Development, research** and **quality inspection**
- **Routine tests** of small batch series and mass production

Technological leader in pulsed inductance measurement for 18 years

www.ed-k.de

Content


ADVENTURES OF OHM
ON BEING AN ENTREPRENEUR
©2020 RIDLEY ENGINEERING INC.

Supporters & Friends

***WE* are here for you!**

Join our free webinars on
www.we-online.com/webinars

The WE-MAPI is one of the world's smallest metal alloy power inductors. Its efficiency is outstanding and now available in new sizes and extended temperature versions with AEC-Q200 Grade 0 qualification for -55° to +150 °C operating temperature in the 4020HT series. Available from stock. Samples free of charge.
For further information please visit: **www.we-online.com/WE-MAPI**

Design your DC/DC converter in **REDEXPERT**, the world's most precise online design platform to calculate AC losses.

- High current ratings up to 10 A
- Low AC losses
- Low DCR down to 6.5 mΩ
- Excellent temperature stability from -55° to +150 °C
- Innovative design
- Excellent EMI behavior

The full WE-MAPI range: 1.6x1.0 2.0x1.0 2.5x0.6 2.5x0.8 2.5x1.0 2.5x1.2 3.0x1.0 3.0x1.2 3.0x1.5 3.0x2.0 4.0x2.0 4.0x3.0 4.0x2.0HT 5.4x2.1 5.4x3.1

A Media
Katzbek 17a
D-24235 Laboe, Germany
Phone: +49 4343 42 17 90
Fax: +49 4343 42 17 89
info@bodospower.com
www.bodospower.com

Publisher
Bodo Arlt, Dipl.-Ing.
editor@bodospower.com

Editor
Holger Moscheik
Phone + 49 4343 428 5017
holger@bodospower.com

Editor China
Min Xu
Phone: +86 156 18860853
xumin@i2imedia.net

US Support
Bob Dumas
Phone +1 516 978 7230
bob@eetech.com

Creative Direction & Production
Bianka Gehlert
b.gehlert@t-online.de

Free Subscription to qualified readers
Bodo´s Power Systems
is available for the following
subscription charges:
Annual charge (12 issues)
is 150 € world wide
Single issue is 18 €
subscription@bodospower.com

Printing by:
Westdeutsche
Verlags- und Druckerei GmbH
Kurhessenstraße 4 - 6
64546 Mörfelden-Walldorf
Germany

Supply Shortages

During the past few weeks we have received several reports of companies increasing their production capacities by buying or taking over factories and production sites. This is a logical consequence of the shortages we have experienced over the past months. The hunger for semiconductors and electronic components often couldn't be met, which may have resulted in a standstill at the customer's factory. There are several reasons for this. First of all, a worldwide pandemic, but also natural disasters, fires in factories or stranded ships in the Suez Canal. What strikes me is that there seems to be a certain trend to look more locally. A way to minimize risks and become more independent, because one thing is clear, the demand will at least remain at the current high level or, more likely, even increase. Future technologies such as the Internet of Things or Artificial Intelligence are in the starting blocks, the acceptance of electro mobility is increasing and there is no way around renewable energies! Good for you and for us, because power electronics is the basis for all of this!

The second edition of Bodo's Wide Bandgap Expert Talk was again a great success. Many thanks to all participants. If you missed it, don't worry. As usual, we recorded the sessions and they are available on our website. We will definitely continue this format, the date for the next talk is already set for September 29. If you have something interesting to say about SiC or GaN and are wondering how you can participate as an expert, feel free to contact us via the usual channels and we will find a way. I can confirm that the format is based on contributions in the magazine!

Bodo's magazine is delivered by postal service to all places in the world. It is the only magazine that spreads technical information on power electronics globally. We have EETech as a partner serving North America efficiently. If you are using any kind of tablet or smart phone, you will find all our content on the website www.eepower.com. If you speak the language, or just want to have a look, don't miss our Chinese version: www.bodospowerchina.com

My Green Power Tip for the Month:
What's good for companies might also be good for individuals. Look local when you buy your services and vacation.

Kind regards

Events

World Battery Expo 2021
Guangzhou, China August 16 – 18
www.battery-expo.com

DesignCon 2021
San Jose, CA, USA August 16 - 18
www.designcon.com

SEMICON Southeast Asia 2021
Singapore & Online August 23 – 27
www.semiconsea.org

IWIPP 2021
Online August 23, 25 & 27
http://iwipp.org

EPE 2021
Online September 6 – 10
www.epe2021.com

PCNS 2021
Milan, Italy September 7 – 10
https://pcns.events

PCIM Asia 2021
Shenzhen, China September 9 – 11
www.pcimasia-expo.com

Industry Tech Days 2021
Online September 13 – 17
www.allaboutcircuits.com/tech-days

The Battery Show North America 2021
Novi, MI, USA September 14 - 16
www.thebatteryshow.com

Changing Name and Corporate Brand

Hitachi ABB Power Grids announced that it will be evolving to become Hitachi Energy from October 2021. The decision to change name has board and shareholder consent and coincides with the business' first-year anniversary since it started operations on 1 July, 2020. Hitachi Ltd. has an 80.1 percent stake in the joint venture and ABB Ltd. holds the balance. Hitachi ABB Power Grids places sustainability at the heart of its purpose: powering good for a sustainable energy future. The transition to the Hitachi Energy name reflects the rapidly evolving energy landscape and the opportunity to create economic, environmental and social value; and with Hitachi enabling the business to position its pioneering and digital technologies to serve existing and future customers, going beyond the grid – opening up a breadth of opportunities in areas like sustainable mobility, smart life, and data centers. By combining advanced digital solutions and services, such as Hitachi Lumada, with an energy platform that is built on unique domain expertise and experience, the business is serving customers and partners co-creating global solutions to solve the global challenge of an inclusive and equitable carbon-neutral future.

Toshiaki Higashihara, Executive Chairman and CEO of Hitachi, said, "With climate change and increasing natural disasters, there is a need to solve three social issues worldwide: environment, resilience, and security and safety." He continued, "Hitachi ABB Power Grids provides a variety of solutions that solve these social issues, and by changing the company name to Hitachi Energy, we are further strengthening our commitment to the realization of a sustainable society."

www.hitachiabb-powergrids.com

Acquiring 300-mm Semiconductor Factory

Texas Instruments announced it signed an agreement to acquire Micron Technology's 300-mm semiconductor factory in Lehi, Utah, for $900 million. "This investment continues to strengthen our competitive advantage in manufacturing and technology and is part of our long-term capacity planning," said Rich Templeton, TI's chairman, president and CEO. The Lehi fab will be TI's fourth 300-mm fab, joining DMOS6, RFAB1 and soon-to-be-completed RFAB2 in TI's wafer fab manufacturing operations. In addition to its value as a 300-mm fab, the acquisition is a strategic move, as Lehi will start with 65-nm and 45-nm production for TI's analog and embedded processing products and be able to go beyond those nodes as required. "The Lehi fab is a great asset and a great team. We are excited about the engineering experience and technical skills the team brings in ramping and manufacturing advanced semiconductor processes," said Kyle Flessner, TI's senior vice president of technology and manufacturing. The companies plan to complete the sale by the end of 2021.

www.ti.com

PCIM Asia 2021 to Feature Over 50 Papers

Asia's leading fair in power electronics will be coming to Shenzhen's World Exhibition & Convention Center from 9 – 11 September 2021, with its renowned accompanying conference to feature guest speakers' talks on a variety of industry hot topics. PCIM Asia Conference 2021 has already confirmed 52 papers from experts in industry and academia to be used in oral & poster sessions, keynotes, tutorials and more during the event focusing on the latest insights and research within the sector.

Held in Shenzhen for the first time on the fair's 20th anniversary, PCIM Asia Conference 2021 promises to once again provide a platform for industry professionals in power electronics, intelligent motion, renewable energy and energy management from around the world to connect and share ideas. For the first time, PCIM Europe conference sessions will be presented at the PCIM Asia Conference in Shenzhen, allowing attendees to acquire industry knowledge exclusively from Europe. The conference will also feature two presentation sessions in Chinese. More information on the aforementioned sessions will be provided on a later date.

The 2021 PCIM Asia Conference will feature a strong line-up of speakers, sharing their expertise through 22 oral presentations and 30 poster sessions. Held concurrently with the conference is the PCIM Asia fair which gathers industry professionals to showcase the latest trends and developments in the power electronics sector, covering a range of power electronics solutions and associated semiconductors, power devices, bus bars, capacitors and more. Recognised as a reputable platform, the exhibition and conference promote industry exchange and development in a professional, international and forward-thinking environment.

www.pcimasia-expo.com

Vertically Integrated Silicon Carbide Production Line

On June 23, Hunan Sanan Semiconductor, located in Changsha High-tech Industrial Park, held its official inauguration to commence its production. Hunan Sanan Semiconductor has a total investment of 16B RMB constructed over a land area of about 667 thousand m2. Since its groundbreaking in July 2020, it has only taken less than a year to build this modern manufacturing facility for the entire silicon carbide compound semiconductor supply chain from crystal growth to power devices, packaging, and testing. A Mega Fab with a monthly output of 30,000 6-inch silicon carbide wafers is now complete and is ready for production.It is the first in China and third in the worldwide industry as a vertically integrated silicon carbide chain, providing customers with high-quality and on-time delivery, while sharing the advantages of large-scale production costs.

The third-generation semiconductor materials have superior electrical properties and can meet the new requirements of power electronics technologies for high temperature, high power, high voltage, and high frequency operation. Through large-scale production and its own silicon carbide material patent portfolio, Hu-

nan Sanan Semiconductor serves a broad range of end markets such as in communications, server power supplies, photovoltaic, electric vehicle (EV) main traction inverters, on-board chargers (OBC), charge piles, smart grids, rail transit and other fields, and is able to realize the widely adopted and popular wide bandgap semiconductor devices.

www.sanan-ic.com

Call for Papers for PCIM Europe Conference 2022

Experts from industry and academia in the power electronics industry are invited to apply to be a speaker at the PCIM Europe Conference 2022 with a short abstract. The Call for Papers will be open until 15 October 2021. The event will be taking place once again on-site in Nuremberg from 10 – 12 May 2022. As a platforms for

exchange in the power electronics community, the event serves as a stage for international speakers to provide their expertise to a qualified audience of around 800 participants. Whether on current developments, the latest research findings or current challenges, speakers are invited to shape the program and share their knowledge in a twenty-minute talk or in a poster presentation. The conference language is English. The PCIM Europe advisory board, led by Professor Dr. Leo Lorenz, ECPE, Germany, will select the papers and also choose the best submissions overall. In addition to the Best Paper and the Young Engineer Award, a further accolade will join the list of prizes: for the first time the main author of one outstanding contribution from academia and research institutions, who is not older than 30 years, will be honored with the Young Researcher Award. Each prize is worth 1,000 Euro. All the papers accepted will be published in the PCIM Europe conference proceedings, as well as in the scientific databases of IEEExplore, Scopus, Compendex and IET Inspec Direct.

www.pcim-exhibition.com

AC Energy Calibration Service Launched

The launch of the service follows Yokogawa's accreditation (K164) to ISO17025, allowing the calibration of AC energy measuring devices at up to 40 MWh at a maximum time of 1000 hours.

This is ideal for manufacturers of products, equipment, or appliances where the measurement of energy efficiency is critical to meet efficiency goals, for proving product specifications or meeting regulatory requirements such as energy labelling of consumer products.

It is also vital for applications for usage-based billing of electrical energy between supplier and user, not only for houses and offices but also for other applications, for example charging of electrical vehicles. Other uses include renewable energy projects such as photovoltaic and wind installations and end tests and type rating where energy is involved.

With the new service, Yokogawa's European Standards Laboratory, based at the company's European Headquarters in Amersfoort, Netherlands, now offers comprehensive energy and power calibration, customized to meet the needs of specific applications.

Erik Kroon, Yokogawa's European Standards Laboratory Manager, says: "We are one of a few laboratories able to calibrate in the frequency range 40 Hz to 1 kHz. "This makes us particularly attractive for engineers working on applications in Automotive, Aviation and Marine and who can now more easily source ISO17025 accredited energy measurements for 400 Hz systems. Using our precise and accurate energy and power calibration services ensures that their designs and instruments meet engineering and quality control requirements."

https://tmi.yokogawa.com

Investing $700 Million to Boost Production Capacity

Nexperia has announced the latest stage of its global growth strategy, confirming a $700 million investment over the next 12-15 months at its European wafer fabs, assembly factories in Asia and global R&D sites. The investment will boost manufacturing capacity at all sites while supporting research and development into areas such as gallium nitride-based (GaN) wide bandgap semiconductors and power management ICs. It will also underpin recruitment activities, with Nexperia looking to attract new chip designers and engineers.

“This is an exciting time in the global semiconductor market, which has mounted a resurgence since the challenges of the first half of last year,” says Achim Kempe, Nexperia’s Chief Operating Officer. “Nexperia reported robust product sales of $1.4B in 2020, with demand accelerating rapidly in Q3 and Q4. That momentum has been maintained so far this year, and we expect it to continue over the long term. The $700 million investment will ensure that we continue to provide the technology and manufacturing capacity needed to deliver products in volumes that support increasing demand.”

As a result, the capacity of the Hamburg fab in Germany – which currently produces more than 35,000 wafers (8-inch-equivalent) per month (70 billion semiconductors per year) – will further increase by 20 per cent from mid-2022. While in the UK, at Nexperia’s dedicated TrenchMOS fabrication facility in Manchester, the capacity will rise by 10 per cent by mid-2022 from the current 24,000 wafers (8-inch-equivalent) per month.

www.nexperia.com

Cooperation to Deliver Silicon Carbide Technologies

EBV Elektronik announced it is working closely with Infineon on the manufacturer’s leading-edge silicon carbide (SiC) based CoolSiC™ technology, which delivers key benefits for engineers designing advanced power systems across a wide selection of market sectors and applications. Infineon and EBV will cooperate over the next year and beyond to accelerate the deployment of energy-efficient power devices with CoolSiC technologies. The CoolSiC portfolio ranges from SiC-based diodes and discrete MOSFETs to hybrid and full SiC modules. “The SiC market is expected to grow at a CAGR of 30 percent over the next 5 years. Infineon is dedicated to participating in this growth for SiC technology leveraging distri-

bution channels that share the same ambition,” said PY Ferrard, Corporate Vice President Distribution & EMS at Infineon. “And we anticipate that EBV can be a cornerstone of our strategy to realise our goals for our CoolSiC portfolio, which provides designers with the ability to realise ever-lower costs and higher efficiency in power conversion systems in fast-growing markets and applications.” “It speaks volumes that Infineon, a world leader in silicon carbide and power technologies, has chosen EBV as its first distributor to run a dedicated programme on CoolSiC technology,” said Thomas Staudinger, President at EBV Elektronik. “It is a clear demonstration of both our know-how and the global reach of Avnet in critically important power electronics applications.” Learn more about EBV’s and Infineon’s joint CoolSiC initiative.

www.avnet.com

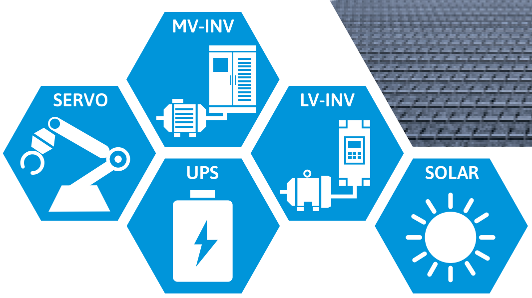

The 7th Generation Modules

DualXT & Premium DualXT

X series 7G

DualXT – Main features

- 7G IGBT & FWD
- New internal layout
- Higher reliability
- Improved silicone gel
- Solder or mini press-fit pins
- More power, lower losses

Premium DualXT – Additional features

- Advanced bond wire design
- High thermal conductive ceramic substrate
- Package material with CTI > 600
- V_{iso} = 4 kV
- High power density

Oscilloscopes Deliver Instant Insights Thanks to Enhanced Usability and Performance

Rohde & Schwarz introduces the next generation of its R&S RTO 6 GHz class oscilloscope. The R&S RTO6 digital oscilloscope offers six different bandwidth models from 600 MHz to 6 GHz and a sample rate of up to 20 Gsample/s. The fully integrated test solution for the time and frequency domain, as well as protocol and logic analysis, supports design engineers from all industries. The instrument features a high waveform update rate, excellent signal fidelity, a uniquely powerful digital trigger and responsive deep memory.

Improved usability for instant insights

When developing the R&S RTO6 oscilloscope, Rohde & Schwarz engineers focused on improving the oscilloscope's everyday usability. They achieved this with a newly designed user interface for increased productivity. The 15.6-inch Full HD screen, with an easy-to-use touch functionality and a redesigned front panel, enables test engineers to quickly set up measurements. The significantly larger screen can display a maximized waveform viewing area, and signals can be dragged and dropped to different parts of the screen with the tried and tested R&S SmartGrid. The app cockpit provides access to all of the oscilloscope's applications with a single tap.

State-of-the-art specifications for in-depth information

The developers of the R&S RTO6 have implemented an architecture with a dedicated ASIC for optimized signal processing that delivers an exceptional acquisition rate of up to one million waveforms per second. This allows users to reliably detect even sporadic signal faults. A low-noise frontend and single-core A/D converters with extremely small linearity errors achieve excellent signal integrity with a spurious-free dynamic range (SFDR) of 65 dBc and an outstanding 9.4 ENOB. This allows users to capture all signal details with maximum precision.

Even more signal details can be revealed using the high definition (HD) mode. This increases the vertical resolution of the R&S RTO6 oscilloscopes up to 16 bit with digital filtering, resulting in sharper waveforms and less noise. This filtered 16-bit signal is also used by the patented digital trigger system from Rohde & Schwarz. This allows the R&S RTO6 to achieve unprecedented trigger sensitivity and the capability to isolate even the smallest signal details.

In addition, the R&S RTO6 has several features that provide users with quick results. Mask tests, which users can set up with simple touch gestures, allow signal anomalies to be easily identified within defined tolerance limits. Thanks to the unique zone trigger, events can be graphically isolated in both the time and frequency domain.

With a standard acquisition memory of 200 Mpts and an optional 2 Gpts per channel, the R&S RTO6 can analyze long pulse and protocol sequences without difficulties. The constantly enabled history mode also allows previous trigger events to be analyzed, while comprehensive search functions further simplify this task.

Comprehensive tools for fast and accurate results

More than 90 measurement functions are included in the R&S RTO6 series, organized into amplitude and time measurements, jitter, eye, histogram and spectral measurements. In addition, multiple application-specific software options for complex measurements are available, and users can easily unlock them with a keycode as their testing requirements evolve, even after purchasing the instrument. These options include triggering and decoding of serial protocols, automated compliance tests on high speed digital interfaces, detailed options for jitter analysis and power analysis, as well as spectrum, power, TDR/TDT and signal analysis. Furthermore, an extensive probe portfolio is available from Rohde & Schwarz to support all measurement tasks with the R&S RTO6. Thanks to its extensive toolset, the R&S RTO6 covers a multitude of applications, ranging from EMI debugging and spectrum analysis to automotive Ethernet testing and serial bus analysis, as well as power electronics testing and digital design.

www.rohde-schwarz.com/product/rto6

Win a Curiosity Nano Evaluation Kit

Win a AVR128DB48 Curiosity Nano Evaluation Kit (EV35L43A) from Bodo's Power and if you don't win, receive a 20% off voucher, plus free shipping for one of these kits.

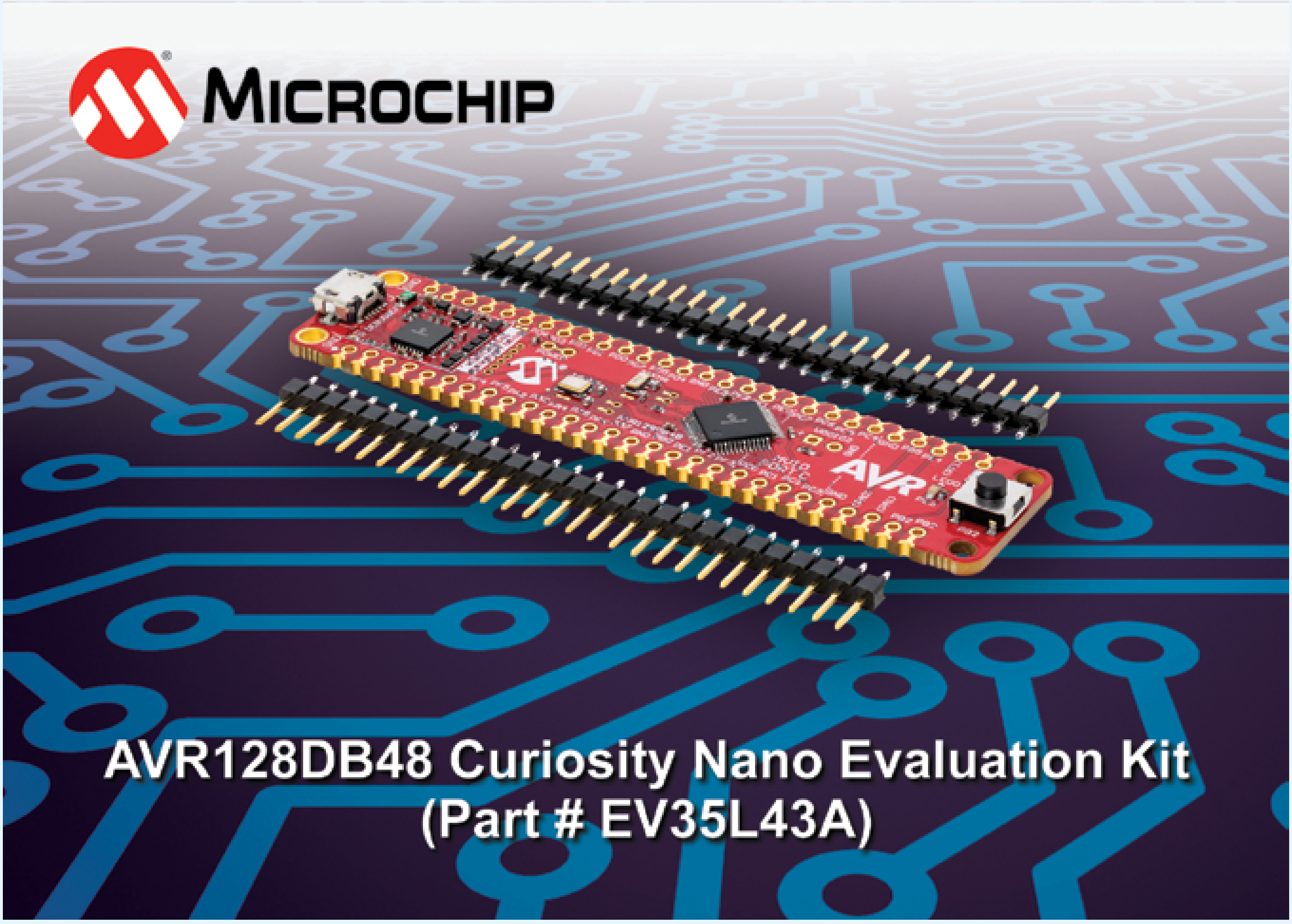

Take your next idea to market with a development board that you can keep in your pocket. With full program and debug capabilities, the AVR128DB48 Curiosity Nano Evaluation Kit offers complete support for your next design.

The AVR DB family of microcontrollers feature the well-known AVR CPU, now running at up to 24 MHz across the full supply voltage range of 1.8V to 5.5V. The family includes 32 KB, 64 KB, and 128 KB Flash variants in 28- to 64-pin package options. The AVR DB family is designed to bring analog signal conditioning, real-time control and multi-voltage operation to applications including industrial control, home appliance products, automotive, and Internet of Things (IoT).

The USB-powered kit features an on-board programmer/debugger that seamlessly integrates with MPLAB® X and Microchip Studio Integrated Development Environments (IDEs). Its small form factor makes the board excellent for breadboard soldering or you can combine it with the Curiosity Nano Base for Click boards™, which features multiple mikroBUS™ sockets so you can easily add sensors, actuators or communications interfaces from Mikroelektronika's extensive selection of Click boards.

This product includes the following features:

- AVR128DA48 microcontroller
- Yellow user LED
- 32.768 kHz Crystal and 16 MHz Crystal
- On-board debugger
- USB powered or externally powered
- Adjustable target voltage

For your chance to win a AVR128DB48 Curiosity Nano Evaluation Kit or receive a 20% off voucher, including free shipping, visit **https://page.microchip.com/Bodo-AVRDB.html** and enter your details in the online entry form.

www.microchip.com

Supply Chain Challenges of the Ferrite Industry as a Result of the Pandemic

Mr. JC Sun, measuring specialist at Bs&T, and Mr. Rico Wachs, from German ferrite manufacturer Tridelta, reflect on the present crisis in the ferrite industry and its challenges amid the pandemic.

By Bodo Arlt, Publishing Editor, Bodo's Power Systems

Following the supply problems of chips and semiconductors, recently passive component supply is also in trouble, especially at the level of the ferrite material and cores. Is it purely a problem of supply or does it also have hidden technical aspects?

JCS: It is both, actually. The enhanced demand on high quality inductive components in Europe and shortage of ferrite supply chain in China is temporally causing a significant asymmetry of demand and supply. But it is much more complex than that, as there are other less obvious technical challenges in the power electronics game.

As I always say: "If magnetics does not get done, nothing gets done!"

RW: China currently represents both the largest producer and consumer ferrite material and cores. There are many manufacturers registered in China, while there are only few in Europe. The high-end market requires specific local presence, while traditional commodity is served by a large number of distributors, who have to fight in different fields. Therefore, we believe that it is a supply bottleneck.

Can you give some example to describe market situation, price and lead time?

RW: We had moderate price increase of less than 5%, with a slightly increase in lead time due to consolidation of location in Hermsdorf and process optimization under one roof. In general, we are talking about 2 to 6 weeks depending on whether the ferrite cores are in stock. Custom designed ferrite cores and small batches from our machining center take 4 to 8 weeks depending on size, shape and quantity, prototypes even only a few working days

JCS: The price of ferrite in China has undergone several readjustments in the order of 25% to 50%, as the raw material price is now uniquely volatile, especially with regards to high purity iron oxide. This segment has almost tripled within half a year. Once the power ferrite is composed of 70% of iron oxide, it determines the price and quality. Manufacturers with material/core validation competence and specialized knowledge acknowledge it, but they represent still the minority.

Is the moderate price increase solely determined by raw material?

RW: Yes, TRIDELTA Weichferrite believes it is. However, we are not only seeing an increase in commodity prices, but also in energy costs. Our process is quite optimized and automatized, and our logistics have not been affected by pandemic, they are still efficient and satisfactory. On the other hand, it is not necessarily true for distributors, who are more directly impacted by logistic uncertainty, such as sharp monthly increases in air and sea freight prices, not to mention the disaster in the Suez Canal. These global parameters have no impact on our core business... what about China Mr. Sun?

JCS: Well, about 40% ferrite manufacturers are buying the ready to press powder as their raw material. It means the ready to press powder is a market for itself; the large technological uncertainty is gradually outsourced to clients, the winding house. Hence, it is not particularly transparent how particularly price increase is allocated in market segments, applications.

The plan uncertainty in price and lead time will have important consequences in the passive component industry, like inductors and transformers, as well many ongoing technological developments - think of DC grid development, ultrafast speed charging, wireless charging and further automotive applications due to electrification - how do you communicate with your clients in this regard?

RW: Absolutely, this is a key issue; we see many developments particularly in magnetization technology. New materials are required to withstand higher temperature, higher Bs material for medium-frequency range, for solid-state-transformer, for infrastructure development. The vulnerability of ferrite industry does exist! Due to large scale offshore activity by larger enterprises, we, as specialist with over 70 years' experience, are looking for sustainable client relationship, focus on high demand products, and serve them with customized application .

JCS: Indeed, experience and competence in validation technique is of essential importance. Since there is no micro magnetic model available to describe the loss behaviour of ferrite, measuring is indispensable not only for core/material quality check, but also for design with multiple gap, and finished potted coil and transformer, for proper specification with limit values for power electronic system performance. I see another consequence, namely on the supply side: the overcapacity will be diminished, and the dependence on China is migrating into the wire wound components industry.

Those 1000 winding houses in Europe are already seeing the challenge. I can only appeal market player in winding industry to validate wire wound component compliant standard, IEC or IEEE, for the sake of sustainable business.

What is your analysis throughout the ferrite chain, and what is your outlook in competition with other soft magnetic materials?

JCS: Ferrite, as artificial ceramic, is almost 100 years old, thanks to pioneer work from Takei and Snoek. This engineering work was continued by Manifer® (TRIDELTA Weichferrite) and Ferroxcube® (Netherlands) after the WWII in Europe. Two major groups of Mn-Znferrite are of interest, power and signal applications, for which low loss and high permeability are mainly important. However, the application with high permeability is facing stiff competition from iron-based nanocrystalline tape wound core as "new kids on the block". Over long term, the technological advantage of inductive component design cored with metallic alloy will win, as the price will decrease due to large economies of scale. A strategy for diversification of material is consolidating, as low-loss materials, withstanding high temperature, is increasingly required for high power/ energy drive application. Therefore, material designers in Europe will in all likelihood need support from local manufacturers, to give a new shape and spirit towards the future ferrite material and core industry.

RW: If ferrite not gets done, nothing gets done, right, Mr. Sun? Our experience in material development and manufacturing of ferrite cores will provide added value to our customers now and in the future.

Thank you both very much for sharing your thoughts!

www.b-stone.de

www.tridelta-ferrite.de

Powering High Performance Computing

Factorized Power Architecture enables next generation processors to achieve their full potential

High performance processors require higher steady state and peak currents with dramatically increasing slew rates, while operating at lower voltages with an increasing number of high speed I/O's. This trend is accelerating and continually challenging power system designers to ensure delivery of adequate power to the processor core with low loss in the Power Delivery Network (PDN).

By Paul Yeaman, Director of Applications Engineering, Vicor Corporation

Conventional approaches utilizing multiphase buck regulators are becoming significantly challenged, rendering a new approach necessary to keep pace.

Vicor's Factorized Power Architecture (FPA™) is a departure from the common multiphase methods and uniquely addresses each of the challenges facing VR developments for new processor technologies. FPA also enables Lateral Power Delivery (LPD) and Vertical Power Delivery (VPD) PCB deployment options. The VPD solution, reduces losses by up to 95% and eliminates bottlenecks by freeing up 100% of the processor perimeter.

Power demands doubling

The rapid advancements in artificial intelligence (AI) are being enabled by advanced GPU's and specialized AI processors utizing the most advanced silicon process nodes at 7nm, 5nm and rapidly on their way to 3nm. Nominal core operating voltages at these process nodes are currently between 0.75V and 0.85V. To meet the performance workloads that AI demands, nominal current consumption has increased, with currents exceeding 600A steady-state and 1000 peak. The trend is a 2x increase from just two years ago and is continuing to rise at a similar rate.

The decrease in voltage and increase in current presents two problems. First, the increase in current exacerbates the copper losses in motherboard PCB's as copper planes and vias connecting the VR to the processor have a constrained resistance. Increasing the processor current increases the losses by the current squared; lowering efficiency and contributing significant additional heat to the processor thermal management system. Secondly, the voltage drop across the PDN is proportional to the increase in current. As core voltage decreases, the effect of this voltage drop has an outsized impact on processor performance.

For example, a core load of 400W with a 100µΩ trace that results in an undershoot of 4% on a 1V rail becomes 7% on a 0.75V rail – nearly 2x greater. The physical constraints of the power delivery network render limited options for reducing that resistance. Adding copper layers or increasing copper thickness to the motherboard will result in lower resistance, but to achieve the same 4% voltage drop at 0.75V, the trace resistance would have to decrease by almost half. Doubling the amount of copper for carrying high current is typically not possible for reasons of cost or physical limitation.

In short, the best solution is to position VR closer to the processor.

While it sounds simple, it is complex to implement. First, there are signal integrity challenges. Moving the hard-switching multiphase VR closer to the processor brings whatever inherent noise the VR has with it. The problem is further compounded by the number of discrete phases needed.

A second challenge is the footprint of the VR. A typical processor package is 60 x 60mm. While that seems large, it is important to note that most of that area is dedicated to I/O. All of the heat is generated in the core, and all of the high currents must find a way to it.

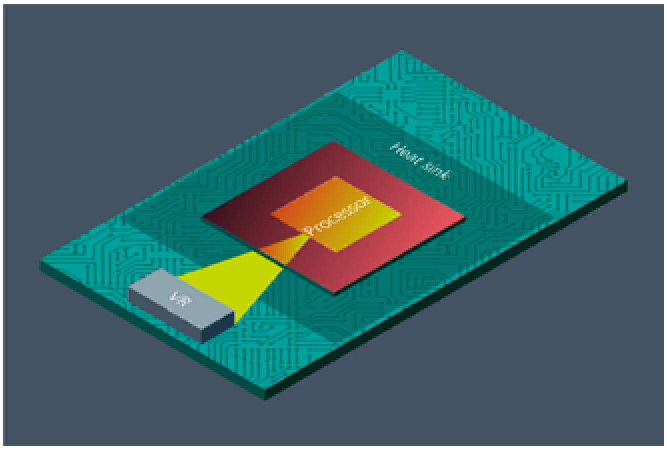

Figure 1: A typical processor package, shown in red, is 60 x 60mm. All of the current is consumed by the core at the center. PCB resistive losses and parasitic capacitance/inductance in the path to the core are what is called the "last inch" and is the limiting factor to ensuring maximum processor performance.

This means that even if the VR is positioned adjacent to the edge of the package, there is still a significant distance that the high current must travel to get to the core. In the typical VR approach, higher current requires more phases. Since most multiphase VRs are discrete devices, the inductor and switching stage must be laid out individually—and in most cases cooled individually as well . Therefore, more phases mean a larger VR that increases the challenge for close placement near the processor.

Factorized Power Architecture unlocks new levels of power efficiency

Factorized Power Architecture (FPA™) is based on the fundamental principle of dividing a power converter into two primary functions, optimizing each separately and then implementing those functions as a system. The two functions are regulation and current multiplication.

Regulation

The efficiency of a regulator is inversely proportional to the work performed – the more work, the lower the efficiency. The closer the input and output voltages of a regulator are to each other, the less work is performed and the higher the efficiency becomes. By virtue of its position in the system, FPA minimizes the regulator's input to output voltage differential. The PRM™ regulator is imple-

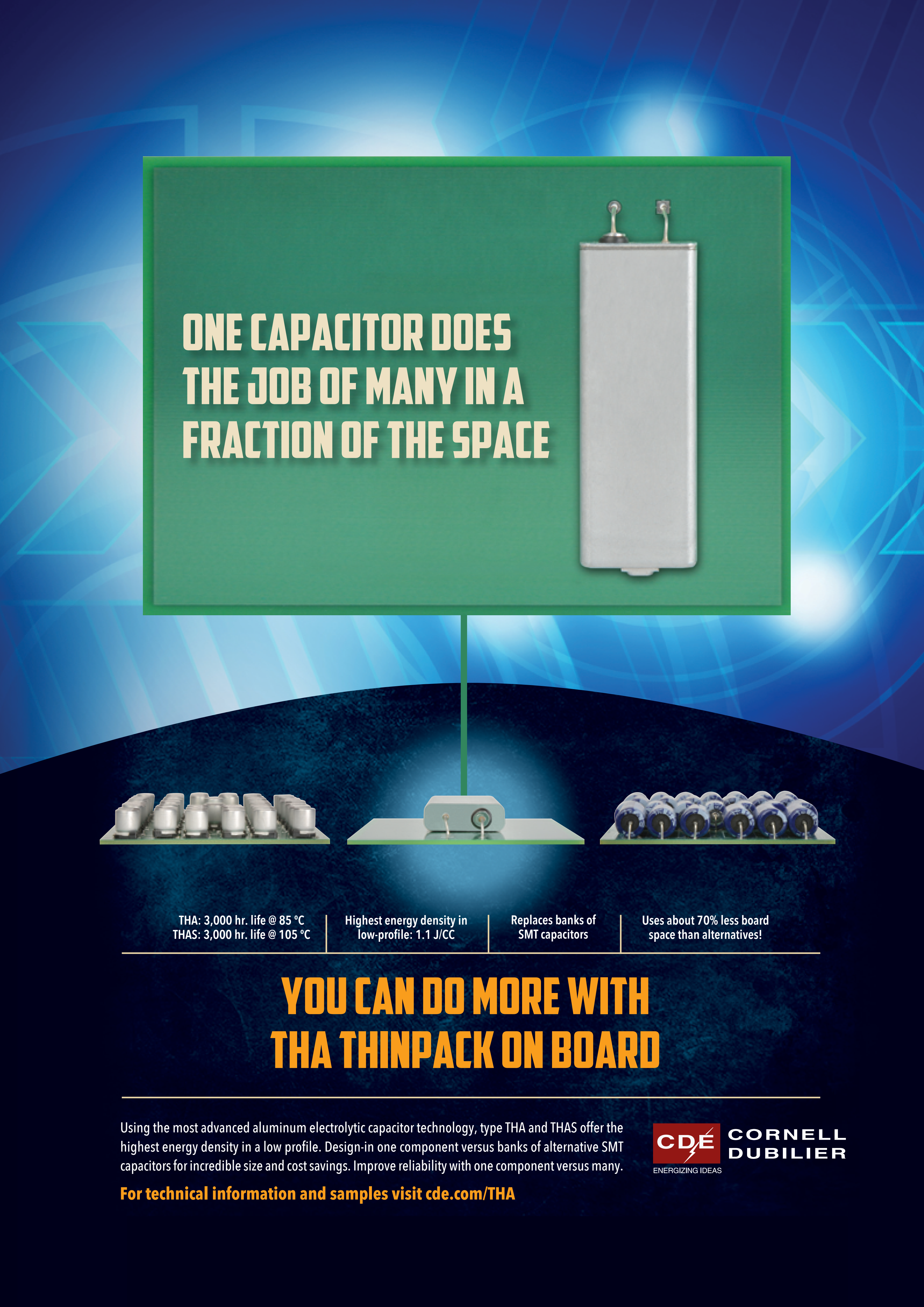
ONE CAPACITOR DOES THE JOB OF MANY IN A FRACTION OF THE SPACE
THA: 3,000 hr. life @ 85 °C
THAS: 3,000 hr. life @ 105 °C
Highest energy density in low-profile: 1.1 J/CC
Replaces banks of SMT capacitors
Uses about 70% less board space than alternatives!
YOU CAN DO MORE WITH THA THINPACK ON BOARD
Using the most advanced aluminum electrolytic capacitor technology, type THA and THAS offer the highest energy density in a low profile. Design-in one component versus banks of alternative SMT capacitors for incredible size and cost savings. Improve reliability with one component versus many.
For technical information and samples visit cde.com/THA
CDE
ENERGIZING IDEAS
CORNELL DUBILIER

mented using a Zero-Voltage Switching (ZVS) Buck-Boost topology, which features high efficiency where the input and output voltage difference is small. ZVS greatly reduces switching losses, enabling high-frequency operation and greatly reducing converter size. The PRM typically regulates an input between 40 and 60V to an output voltage between 30 and 50V.

Current Multiplication

The PRM is followed by a second stage performing a voltage step-down and current step-up function. This is implemented using the Sine Amplitude Converter topology in a device called a VTM™ Current Multiplier. The VTM's behavior can be realized as an ideal transformer, where the input and output voltage are related by a fixed ratio and the device impedance remains low (hundreds of μΩ) beyond 1MHz.

Since there is no energy storage in the VTM, it can provide large amounts of power if it is kept sufficiently cool. This allows for matching the power capability of the VTM with the thermal capability of the processor. Together, the PRM and VTM form the building blocks of FPA.

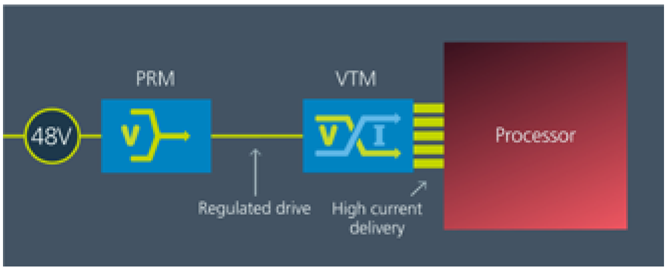

Figure 2: PRM™ and VTM™ are the building blocks of FPA. PRMs are selected based on the system input voltage range and power requirements; VTMs are selected based on the output voltage range and current requirements. The PRM can be mounted anywhere in the system where convenient; the VTM should be mounted as close to the processor core as possible.

One is dedicated to regulation followed another dedicated to transformation.

SM-ChiP package reduces noise and improves thermals

While the topology and architecture used to implement a high-performance regulator are important, of equal importance is the packaging technology. Vicor's SM-ChiP package integrates everything – passives, magnetics, FETs and control – into a single device. Moreover, this package is engineered to enable the most efficient extraction of current at the lowest thermal impedance to facilitate cooling. Many SM-ChiPs also include grounded metal shielding

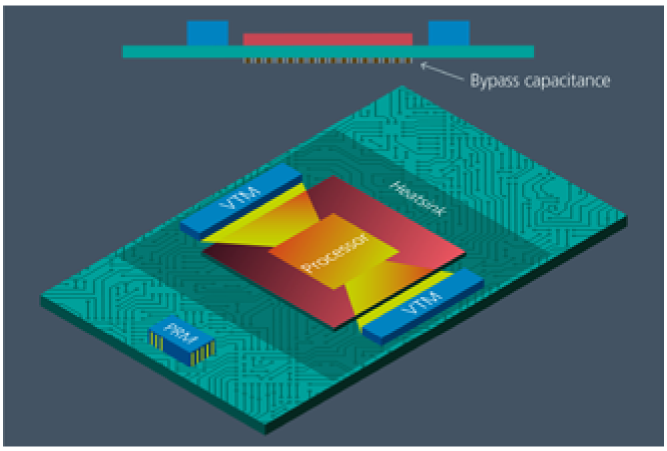

Figure 3: Typical PRM/VTM Factorized Power Architecture solution supporting main rail power on an AI accelerator card. Placing VTMs on opposite sides of the socket divides current flowing through the power delivery network to the processor in half and reduces losses by 50%.

over a significant surface of the device. This serves not only to facilitate cooling but also to localize high-frequency parasitic currents to keep them from propagating outside the device.

Lateral power delivery cuts PDN losses by 50%

To provide flexibility for a wide variety of application implementations, Vicor has developed PRMs and VTMs with power level granularity that enables flexibility to support reducing PDN loss. For example, implementing a single higher-current VTM as two smaller lower-current VTMs allows for placement on opposite sides of the processor socket. This reduces power delivery network losses by 50%, dividing the current in half and adding a separate path to the core area.

At 2.8mm, the VTM is thinner than many of the mechanical processor support elements such as package sockets, stiffeners and heat sink attachment hardware. Locating the VTM under these elements couples them to the processor thermal management system and eliminates the need for a dedicated VTM heat sink while at the same time reducing power delivery network losses by locating the current multiplier closer to the core.

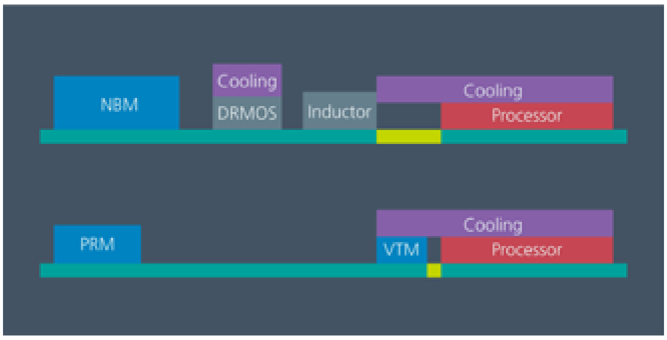

Figure 4: In a typical multiphase VR, the phase inductor height typically limits its proximity to the processor and separate cooling is required for the DRMOS stage. The low profile of the VTM allows it to move under the processor heat sink and associated hardware, while PRM can be placed farther away without loss in performance.

These are examples of lateral power delivery (LPD). In LPD, the current multiplier is located on the processor side of the motherboard and the current flows laterally from the VR to the processor. This presents an inherent loss no matter how close the current multiplier is to the processor core.

The solution to this inherent loss is vertical power delivery (VPD). In VPD, the current multiplier is located on the opposite side of the processor, directly underneath it.

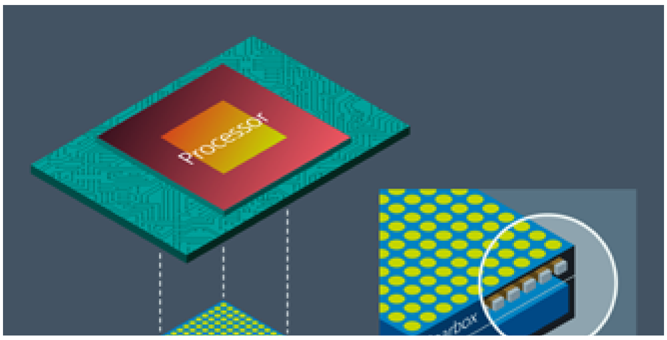

Figure 5: Vertical power delivery (VPD) with GTM Geared Current Multiplier placed underneath processor maximizing power delivery performance. The VPD solution also relieves the processor top-side periphery for options including higher I/O routing, onboard memory, or tighter processor clustering.

Significantly reducing PDN losses by reducing the distance the current travels through the motherboard. VPD needs two key features to achieve this function.

First, the area directly under the processor contains high-frequency capacitors which are necessary to decouple very high-frequency currents (>10MHz) from the rest of the system. Secondly, for maximum efficiency, the physical location and pattern of the current exiting the VPD solution must exactly mirror the location and pattern of the processor core power inputs. This enables the high-current flow to achieve a true "vertical" profile.

To achieve these features, the Vicor VPD solution consists of VTM Current Multipliers implemented with a gearbox to comprise a GTM™ Geared Current Multiplier. The gearbox performs two functions: it incorporates the high-frequency decoupling capacitance and redistributes the current from the VTM into a pattern mirroring the processor above it. The VTM array in a GTM is sized based on the processor output current requirement and the gearbox BGA pattern is based on the processor. In this way, the GTM represents the combination of both a standard (VTM) and a customer (gearbox) solution.

A better way for high performance computing power

The implementation of Factorized Power Architecture LPD and VPD solutions using SM-ChiP packaging enables sweeping reductions in power delivery network losses for low-voltage, high-current processors. As processor current requirements continue to climb to 1000A and beyond, the Vicor Factorized Power Arcitecture will be able to deliver lower core voltages and higher core currents while providing lower power delivery network losses and higher system efficiency.

www.vicorpower.com

Attaining Highest PFC Efficiency by Moving from IGBT to SiC

The continuing worldwide efforts to reduce carbon emissions have driven the growth in interest in electric vehicles (EV). As a result, the demand for a refuelling infrastructure to recharge them is also increasing. Over the course of a few years, millions of charging points capable of delivering between 3.6 kW and 22 kW will be installed, with fast-charging solutions peaking at 150 kW.

By Matthias Ortmann, Chief Engineer, Application Support, Semiconductor Marketing, Toshiba Electronics Europe

Not only must this massive increase in load be supplied and managed, but the charging solutions installed must also play their part by making use of the latest technology to attain the highest possible efficiencies and unity power factor (PF). Power Factor Correction (PFC) stages have been standard in electrical equipment since the European Union established limits on harmonic currents. Power supplies with an input power of 75 W or greater must conform with EN61000-3-2.

Furthermore, market demands are placing pressure on the volume of design and heat dissipation, with a general trend to move towards passive cooling where possible. This puts pressure on designers to find more efficient approaches to their power converter designs. Until recently, PFCs have been the domain of silicon IGBTs, leveraging their high VCES, current handling capability, and robustness. However, the introduction of wide-bandgap power devices is changing the way PFCs are implemented.

Silicon carbide MOSFETs for PFCs

Wide-bandgap technologies, such as silicon carbide (SiC), open up a range of new possibilities for the designers of power converters. Compared to existing IGBT devices, SiC offers significant reductions in turn-on and turn-off losses, as well as improvements in conduction and diode losses. Careful analysis of their switching characteristics shows that SiC MOSFETs fully turn on almost immediately, whereas IGBTs display a significant slope by comparison. This results in a substantial drop in Eon energy losses.

Operating a fast-switching IGBT and Toshiba TW070J120B SiC MOSFET under the same laboratory conditions showed that switching losses in the SiC MOSFET lay at 0.6 mJ. This was around a quarter of the 2.5 mJ measured for the IGBT. In each case, testing was undertaken at 800 V, drain/source current of 10 A, ambient temperature of 150 °C, and optimal gate-emitter threshold voltages (Figure 1).

Simulated in a 3-phase, 400 V PFC, the SiC MOSFET shows application benefits over the IGBT. Factoring in all switching losses, on-

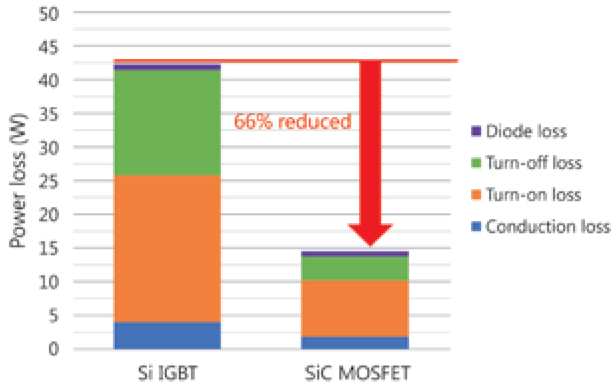

Figure 2: Implemented in a 3-phase PFC, the SiC MOSFET shows a 66% reduction in power loss compared to an IGBT-based design.

resistance related conduction losses, and forward voltage loss of the internal diode, a SiC MOSFET-based design saves around 66% in losses over a comparable IGBT-based design (Figure 2). This efficiency improvement provides designers room to reduce the volume of their PFC designs if designing to deliver the same power, or increase power in a design of the same volume.

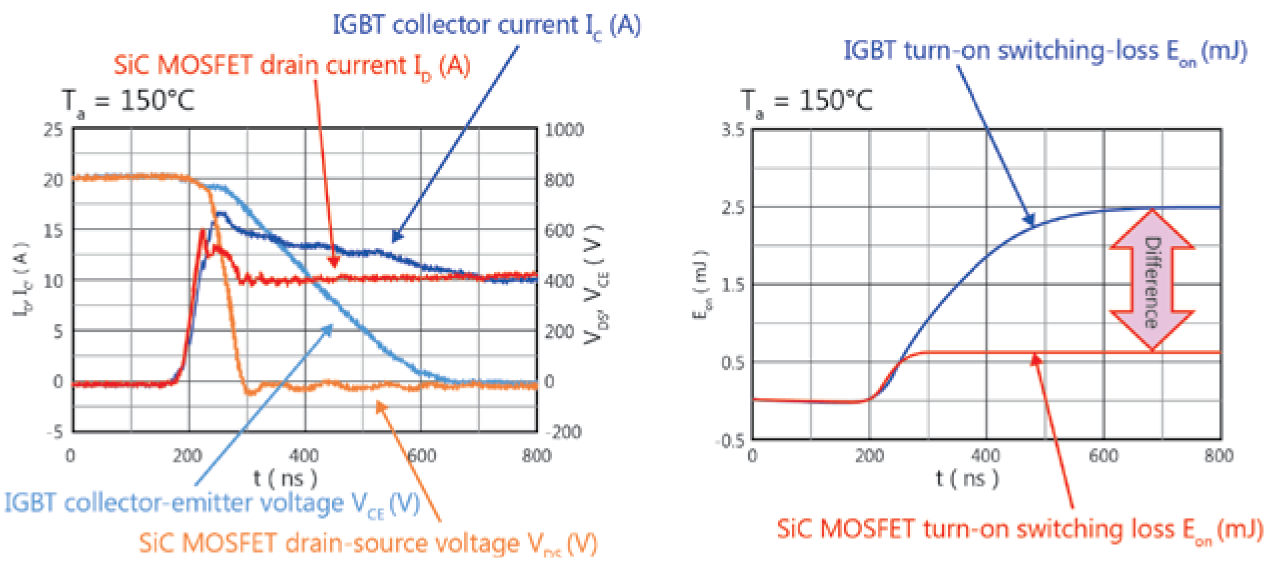

Figure 1: Compared to latest-generation IGBTs, the TW070J120B SiC MOSFET shows considerably faster switching speeds that deliver higher efficiencies in power converters.

The integrated diode of the TW070J120B provides an excellent forward voltage (VDSF) of just -1.35 V (typical) that is also very robust to current surges, handing current pulses of up to 72 A (TC = 25 °C). The -10 V to 25 V gate-source (VGSS) is wider than competing products, facilitating easier design, while the high gate threshold (Vth) of 4.2 to 5.8 V protects against unwanted switching due to gate voltage fluctuations and noise.

Accelerating SiC-based PFC design

While the move from silicon IGBT to SiC MOSFET in power converters is relatively straightforward compared to other Wide Band Gap (WBG) technologies, access to reference designs is universally recognised as being the fastest way of mastering new technologies. The Toshiba 3-phase, 400 V AC input PFC reference design has been specifically designed with applications such as EV charging in mind (Figure 3).

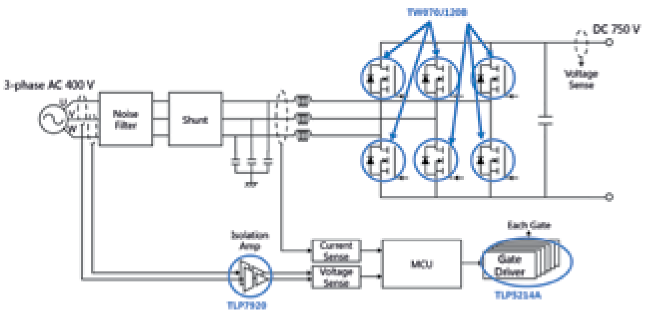

Figure 3: The TW070J120B SiC MOSFETs are coupled with the TLP5241A gate driver in Toshiba's 3-phase, 400 V PFC reference design.

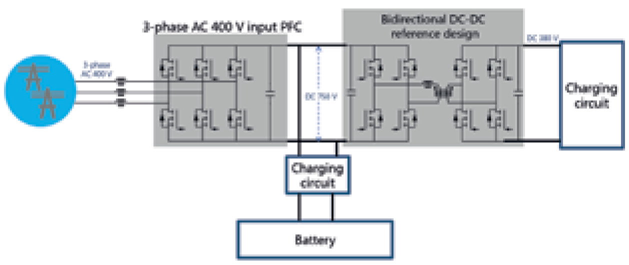

Figure 4: The Toshiba 3-phase, 400 V PFC reference design is ideal for use with bidirectional DC-DC converters in battery charging applications.

Generating a 750 V DC link output, it achieves a conversion efficiency of 97% and a power factor of 0.99 or better. It uses a bridgeless 3-phase totem pole design, switching each phase directly from a 50 or 60 Hz line of between 312 V AC and 528 V AC. The design is suited for use with bidirectional DC-DC converters to implement EV battery chargers for which a further reference design is currently being developed (Figure 4).

The reference design couples the 1200 V TW070J120B SiC MOSFETs with the TLP5214A gate drivers to attain optimal performance. This allows switching frequencies of 50 kHz to be used, higher than those allowed by IGBTs, leading to a reduction in both the size of the inductors and power converter. The higher switching frequency can lead to challenges in fulfilling EMI requirements. Gate drive circuit switching speed can, however, be easily tuned, albeit at the expense of overall efficiency.

Critical to optimal control of SiC MOSFETs is the application of the correct gate signal, and it is essential to adhere to the application of gate voltages as defined in the datasheet. The reference design ensures that this always lies between the specified -10 V and 25 V. The turn-on voltage is set to lie between 18 V and 20 V, while the turn-off voltage is configured for between 0 V and -5 V.

At turn-on, the gate requires 70 nC, so the gate driver must be capable of providing this energy at the switching frequency selected. The TLP5214A used comfortably sinks and sources up to 4 A, which is enough to drive and discharge the gate of the TW070J120B. Additionally, it is equipped with overcurrent and undervoltage lock-out protection for robust handling of system abnormalities.

Summary

The rapid adoption of EVs is bringing the challenges of keeping them fuelled into sharp focus. With the high-power levels involved, every percentage point of inefficiency results in hundreds of Watts of wasted energy. While IGBTs have traditionally been relied upon for the bulk of active PFC designs, next-generation designs demand higher performance that pushes efficiency to the limit of what is possible. SiC, a robust and high-voltage-capable WBG technology, is displacing IGBTs in such applications. Thanks to carefully designed reference designs, such as Toshiba's 3-phase, 400 V PFC, engineers are able to not only quickly evaluate such designs but also acquaint themselves with SiC MOSFET technology, allowing them to develop stable and reliable power converters rapidly.

www.toshiba.semicon-storage.com/eu/semiconductor

Troubleshooting Common-Mode-EMI in Electric Drive Installations

This article sketches the basic principles and origins of CM currents and uses a case study to show the measurement concepts and counter measures required to conquer CM signals in electric drive installations.

By Dr. Markus Herdin, Market Segment Manager Industry, Components, Research & Universities at Rohde & Schwarz

Introduction

Common mode (CM) signals frequently occur in variable-frequency drive installations. Especially the high-frequency common mode voltages introduced by the converter lead to capacitive CM currents flowing from stator windings to ground through different paths of the machine. This not only stresses the different insulation layers, but also severely damages the bearings of the motor, leading to significant reduction in the machine's lifetime.

Common Mode Noise

Based on the individual line voltages of the electric drive output, the common-mode component of an electric drive output can be calculated by

$$V_{CM} = \frac{1}{3}(V_a + V_b + V_c), \quad (1)$$

which is identical to the zero sequence component when using symmetric components [1] [2].

While low frequency CM harmonics can be controlled by adapted modulation schemes, the high-frequency components driving the CM current flowing through the machine highly depend on the different components themselves, but also their mutual interaction and different installation parameters. Minimizing high frequency CM noise therefore often requires to additionally optimize the system after installation.

Even though there is no explicit CM path in most applications, parasitic capacitances, as shown in red in Figure 3, allow for common mode currents if CM voltages are present.

In real setups, mostly neither the stray capacitances nor the line or load impedances are identical. Thus, the common-mode voltage will lead to a current distribution with $I_{L1} \neq I_{L2} \neq I_{L3}$, resulting in different voltage drops across the nodes of the load which are measureable as differential-mode disturbances. This phenomenon is hence called common-mode differential-mode (CMDM) conversion. Analogously, it is also possible for DM disturbances to be converted into CM signals (DMCM conversion).

Note, that also EMI-filters, which are usually inserted between line and converter or line and load, can lead to CMDM or DMCM conversion [3] [4].

Problems with Common Mode Noise in Power Drive Systems

Besides the need to meet the EMC standards for power drive systems [5], CM signals may cause severe damages to the machine. As can be seen in Figure 1, a certain portion of the CM currents flow from the stator windings towards the rotor via parasitic capacitances. While one part (blue) of the CM current directly flows to ground via the capacitance between stator winding and stator itself, another part flows to the rotor via the stator-winding to rotor capacitance . From here, the current will either flow to ground via the stator-rotor capacitance (green) or take the path through the bearings of the machine (yellow).

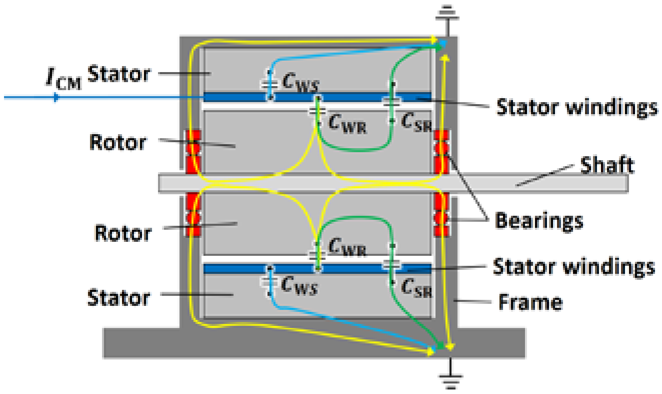

Figure 1: Different current paths for high-frequency CM currents induced to the machine by the converter.

Due to the lubricant insulation film building up at high rotor speed (n>100/min), the bearing impedance is mainly capacitive. However, random contacts or dielectric breakdowns lead to sudden discharge effects of these capacities via the spheres inside the bearings. This results in high currents flowing through the contact point between the bearing ball and the races, causing fluting, scoring and cracks or fractures. These damages accumulate over time, leading to bearing failure eventually and reducing the lifetime of the machine drastically, involving high costs due to downtimes [6].

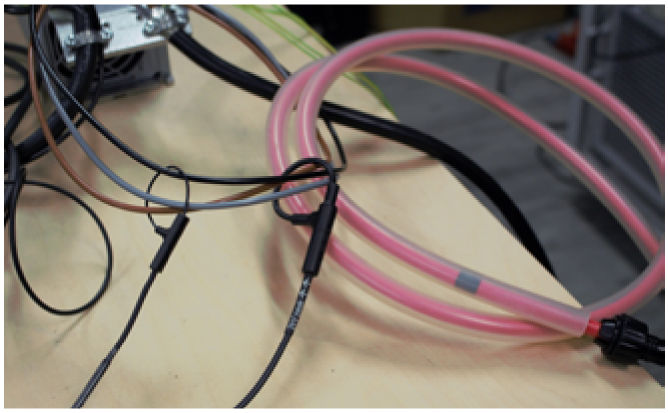

Figure 2: Measurement of CM current with three different Rogowski coils from PEM UK [8] - left: PEM CWT Ultra mini, middle: PEM CWT miniHF, right: PEM custom made (2 windings)

Measuring CM signals

The CM current can be easily and accurately measured on site using handheld oscilloscopes like the R&S RTH1004 in combination with high-bandwidth Rogowski coils [7]. Here, the CM current can directly be measured by closing the Rogowski coil around all three phases, as shown in Figure 2. We note that it is crucially important for a valid measurement to exclude the cable screen from the measurement, as shielding currents will otherwise influence the measurement. As schematically shown in Figure 3, this can usually simply be realized directly at the converter output ① or at the machine input ②.

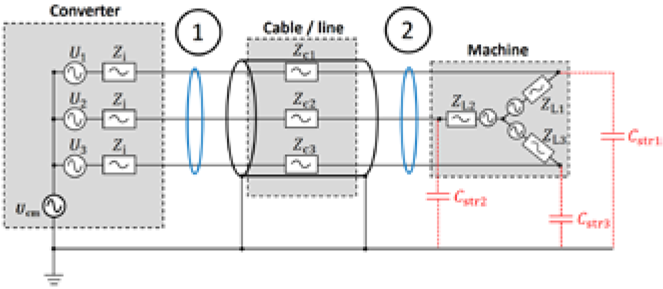

Figure 3: Measurement of CM current using Rogowski coils (blue) either at the converter output ① or at the machine input ②

The high-frequency CM current signals usually consist of pulse patterns. It is important to carefully adjust the trigger to the peak-value. Otherwise, the oscilloscope might display a maximum value lower than the actual one. This is on of the most frequent reasons for underestimations of CM currents.

Counter Measures

An efficient way to reduce the CM currents flowing into the machine is to increase the common mode impedance. This can efficiently be achieved with current compensated chokes. Here, all three phases are fed through high permeability ring cores. Since the differential currents are cancelling out, the choke introduces an impedance for the CM current only.

Figure 4: Four high-permeability ring cores are connected in series as current compensated chokes with 2 windings in total.

Depending on the application, a certain ring-core geometry, material and number of windings is to be used to sufficiently increase the CM impedance of the choke. For the right choice of the core, tables [9] [10] or online simulation tools [11] can be used. In Figure 4, four high-permeability ring cores from MAGNETEC were used as current compensated chokes with two windings each. The effect of these measures is displayed in time domain in Figure 5. As can be seen, the peak-value is reduced from 13.77 A to 3.15 A, which is more than a factor of four.

Another useful way to visualize the effect of the applied counter measures is the FFT function of the oscilloscope, as it directly allows to investigate the effect of a specific measure on the frequency range of interest. Figure 6 shows the effect of the four chokes displayed in the frequency domain, using the oscilloscopes FFT-function.

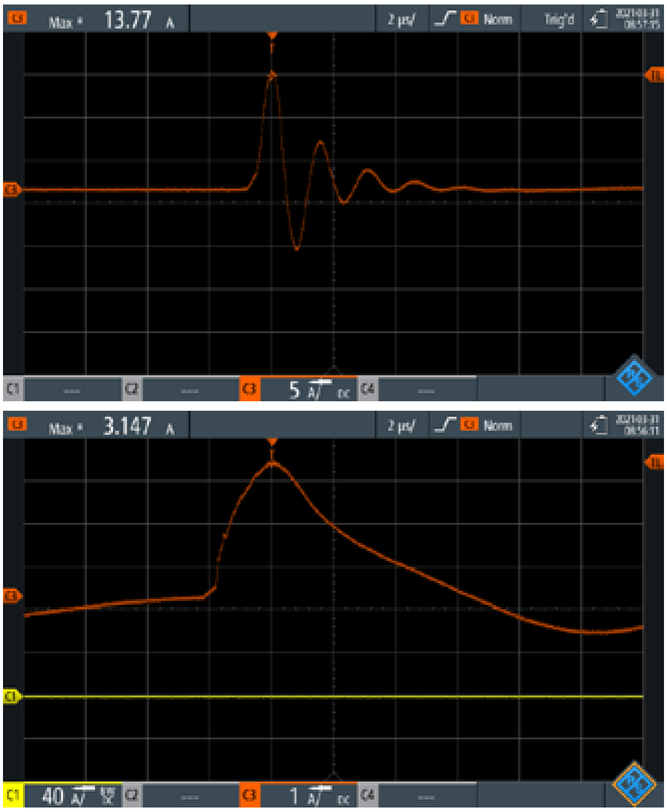

Figure 5: Typical CM-current pulse pattern without counter measures (upper screen) and after the injection of current chokes (lower screen)

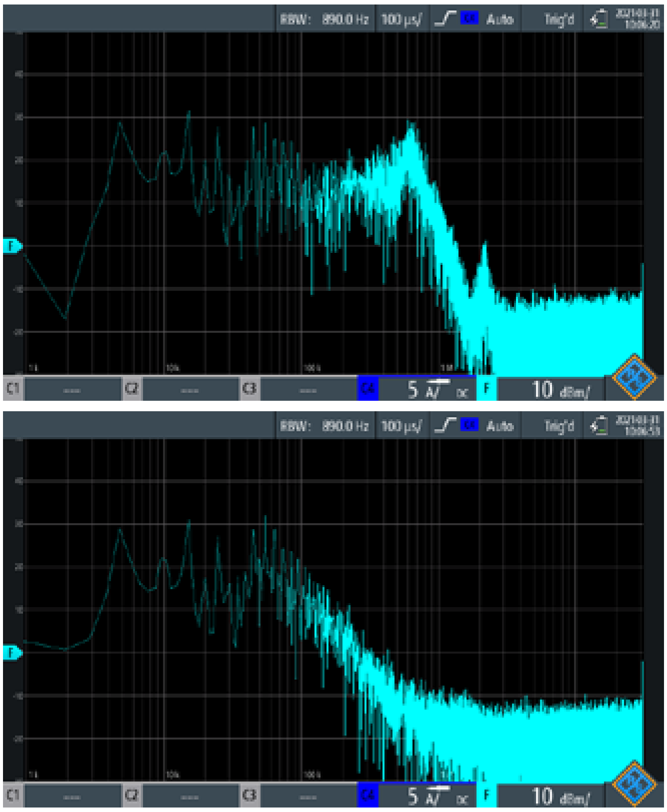

Figure 6: Visualization of the frequency of the CM current using the FFT-function of the oscilloscope. The spectrum before the insertion of the chokes is shown on the left, the spectrum after the insertion is shown on the right side.

The measurement of the frequency spectrum becomes especially important since every EMI-filter including current compensated chokes introduces new energy-storage components in form of capacitances or inductances, which can cause additional oscillations, resonances or even instabilities. Therefore, the effect of filter elements on the system behaviour should thoroughly be measured for all operation points.

Summary

Common mode (CM) currents are one of the main causes for bearing failures and can thus significantly reduce the lifetime of electric drives. Therefore, CM interferences need to be thoroughly investigated after installation on site. Here, handheld oscilloscopes in combination with Rogowski probes are powerful tools to easily determine these CM currents and to measure the effect of counter measures. In this article, the measurement of CM quantities is shown in addition to the insertion of current compensated chokes (CCC) as an affective counter measure. The measurements show that the usage of four magnetic ring-cores acting as CCCs, the peak current is reduced by more than a factor of four.

Sources

[1] C. L. Fortescue, „Method of Symmetrical Coordinates Applied to the Solution of Polyphase Networks," AIEE Transactions, Volume 37, Part II, pages 1027-1140, Atlantuc City, USA, 1918.

[2] C. F. Wagner und R. D. Evans, „Symmetrical Components," McGraw-Hill Book Company, New York, USA, 1933.

[3] Y. M. a. A. N. Mamoru Kamikura, „Investigation on the mode conversion between common-mode and differential-mode noises in EMI filters for power electronics circuits," Proc. of the 2013 International Symposium on Electromagnetic Compatibility, Brugge, Belgium, 2013.

[4] S. Wang und F. C. Lee, „Investigation of the Transformation Between Differential-Mode and Common-Mode Noises in an EMI Filter Due to Unbalance," IEEE TRANSACTIONS ON ELECTROMAGNETIC COMPATIBILITY, 2010.

[5] IEC 61800-3, „Adjustable speed electrical power drive systems - Part 3: EMC requirements and specific test methods".

[6] „Avoid Motor Shaft Voltage & Bearing Current Damage," Renown Electric.

[7] Rohde & Schwarz, „How to Measure and Reduce Common Mode disturbances in Electric Drive Installations," White Paper, https://www.rohde-schwarz.com/de/applikationen/..., 2021.

[8] P. UK, „Rogowski and Current Measurement," [Online]. Available: http://www.pemuk.com/.

[9] MAGNETEC, „Nanoperm - Cased EMC Core Selection Matrix," [Online]. Available: https://www.magnetec.de/wp-content/uploads/2020/04/Cased_EMC_Core_selection_matrix.pdf.

[10] MAGNETEC, „CoolBlue - Tape Wounded Cores to Reduce Motor-Bearing Currents," [Online]. Available: https://www.magnetec.de/wp-content/uploads/2021/01/CoolBlue_NaLA.pdf.

[11] MAGNETEC, „Magnetec Simulation Tool," [Online]. Available: https://mgntc.pe-finder.de/.

www.rohde-schwarz.com

DC/DC Converters Optimized for Energy Storage Elements in Smart Grid Solutions

DC/DC converters are a core element in renewable energy production and storage unit management. Putting numerous demands in terms of reliability and safety, their design is a challenging task of fulfilling many competing requirements. In this article, we are on the quest of a solution that combines answers to these questions in one single device.

By Kristina Schmidt and Willi Spiesz, Grau Elektronik GmbH, Karlsbad

Introduction

The energy transition is on the rise. The proportion of renewable energy sources such as wind power or photovoltaic energy is growing. On the opposite, stable electric power supply and availability have to be guaranteed at any time. This undeniable fact raises the question of energy storage in future decentralized energy systems. Storing energy in the form of current or voltage means to use higher voltage levels in order to benefit from higher efficiency. Therefore, powerful DC/DC converters are needed for bringing the voltage down to another level, in order to provide auxiliary voltages for control electronics (figure 1). On the other hand, the way towards a smart grid, that is able to retrieve energy when needed, calls for availability round the clock. Monitoring features, control unit functions and communication modules with energy supply companies have to work reliably, for the energy storage elements as well as for the primary energy production itself: As an example, a wind turbine, producing voltages up to 3000 V, needs an underlying supply voltage to be set in motion at all. So DC/DC converters will be found anywhere in the countryside.

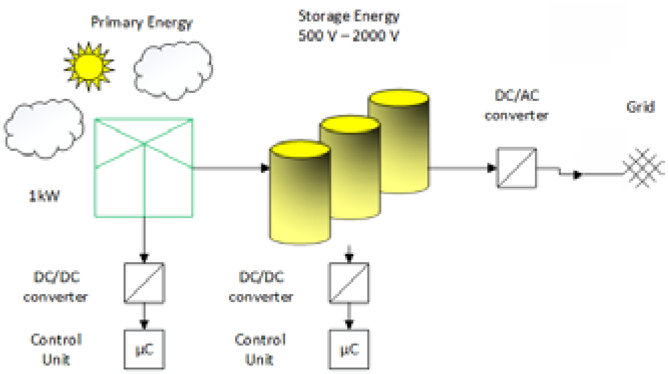

Figure 1: DC/DC converters in application

High requirements guarantee maximum grid stability

DC/DC converters are largely used in today's electric devices, they are indispensable in the use of household or entertainment appliances. However, in most cases, these devices are designed for the use in low voltage range. They usually convert down from line voltage level to 5V, 15V, or 24V. Hence, they are conceived for this specific operating condition. They have to take into account a number of constraints that concern insolation, cooling and reliability issues. Given their limited input range, these challenges are easy to be dealt with.

But considering now a use for MVDC (medium voltage DC) applications, as it is the case for energy storage elements or renewable energy plants, the requirements are increasing. For safety reasons, insulation gains in importance as the input voltage might go up to 1000V, 2000V or even higher for some use cases. On the opposite, the higher the voltage, the more difficult is the process to guarantee an insolation proof construction of the material in use. In addition, given the importance of supply security in the energy grid, a maximum of reliability is required. Considering the very complex interdependences of today's energy grids, the failure of such a DC/DC module, integrated anywhere in the supply line, can cause the breakdown of the whole system with all negative consequences for consumers. In conclusion, confident solutions to limit EMC impact and to ensure galvanic separation have to be found. Nevertheless, the operating conditions of such devices are far to be comparable to those applied to conventional DC/DC converters, like flyback converters conceived for low voltage context. Renewable energy is caught there where local conditions are most favourable, like on mountains or other areas where extreme conditions are prevailing. Hence, high altitude, corrosive impact and inconvenient temperature have to be taken into account. On the other hand, efficiency issues have high priority. So what would this mean for such a MVDC application under real conditions?

On the track of parasitic elements

Following the logic that higher voltages are beneficent to energy storage applications as energy is growing proportionally to voltage squarred, let us look at a small example concerning the DC/DC conversion mentioned above. We take the equation $W = 1/2 \times C \times U^2$ as a basis. However, in real life applications, power losses during the transformation cannot be avoided. Voltage drop regulation is no longer option in most cases. Consequently, the voltage will be clocked to transfer the power from primary to secondary side in order to limit these losses. Anyway, parasitic elements come to disturb the efficiency of such an application, as the distances between primary and secondary side will be increased. Parasitic elements can be found all over the process that leads to the DC/DC conversion. There is a certain number of additional elements that make their contribution, as the transistor, the heatsink, the transformer itself and the diode:

$C_{par} = C_{oss} + C_{Heatsink} + C_{Transformer} + C_{Diodereflect}$.

Considering this for a typical Fly Back converter, we have to accept that the parasitic capacity recharges when the transistor is switching through for a moment. When switching over the transistor due to clocking, the capacitor will discharge by a short circuit and heat will be released. Let us see what will be the differences in use between the DC/DC converter conceived for low voltage application and the one designed for MVDC context.

Power losses reaching a higher dimension

We take as an example a parasitic capacity C_{par}= 250 pF for a very first estimation and a switching frequency f_{sw} = 60 kHz. For the low voltage case, we assume an input voltage V_{in} = 110 V, an output voltage V_{out} = 25 V (24 V + V_{Diode} = 24 V + 0.7 V ≈ 25 V) and a duty Cycle DC = 0.5. Out of that, we can first calculate the turns ratio

needed for holding the energy balance inside the transformer and then the drain voltage V_{DS} of the transistor:

$$\frac{V_{in} \times t_{on}}{n_{prim}} = \frac{V_{out} \times t_{off}}{n_{sec}} \Rightarrow \frac{n_{prim}}{n_{sec}} = \frac{V_{in} \times t_{on}}{V_{out} \times t_{off}}$$

$$t = \frac{1}{f}$$

$$t = \frac{1}{60\ kHz} = 16\ \mu s$$

$$t_{on} = t_{off} = 0.5 \times t = 8\ \mu s$$

$$\frac{n_{prim}}{n_{sec}} = \frac{110\ V \times 0.08\ ms}{25 \times 0.08\ ms} = 4.4$$

$$V_{DS} = V_{in} + \frac{n_{prim}}{n_{sec}} \times V_{out}$$

$$V_{DS} = 110\ V + 4.4 \times 25\ V = 220\ V$$

Concerning the power losses, we get already an idea of what will be the switching losses caused by the parasitic elements:

$$P_{loss,par} = \frac{1}{2} \times C \times U^2 \times \frac{1}{t}$$

$$P_{loss,par} = \frac{1}{2} \times 250pF \times (220\ V)^2 \times \frac{1}{16\ \mu s} \approx 0.36\ W$$

Speaking for an output power of 250 W, this will only be about 0.15%. So they seem to be negligible at a first glance. In comparison, transistor conduction losses, caused by the inner resistance of the transistor when switched on, will matter to a larger extend. As an example, we will consider an effective current $\hat{I}_{Trs}$ = 9 A for a TO-220 600 V transistor with a switch-on resistance $R_{ds,on}$ = 0.1 Ω @ + 100 °C:

$$P_{loss,con} = \hat{I}^2 \times \frac{DC}{3} \times R_{DS,on} \times \frac{1}{t}$$

$$P_{loss,con} = (9\ A)^2 \times \frac{0.5}{3} \times 0.1\ \Omega \times \frac{1}{16\ \mu s} = 1.35\ W$$

So this will be about 0.55% of the output power and almost four times the power losses caused by parasitic elements.

However, considering now a medium high voltage system with an input voltage V_{in} = 1000 V, we can see that power losses matter to a very larger extend:

$$\frac{n_{prim}}{n_{sec}} = \frac{1000\ V \times 0.008\ ms}{25 \times 0.008\ ms} = 40$$

$$V_{DS} = 1000\ V + 40 \times 25\ V = 2000\ V$$

$$P_{loss,par} = \frac{1}{2} \times 250pF \times (2000\ V)^2 \times \frac{1}{16\ \mu s} \approx 30\ W$$

As we can see, this makes already 12% of the output power. Hence, the flyback converter is unfavourable in this particular application because the reflected voltage will be added and worsen the parasitic effect. The first step towards minimizing these undesired effects will be the use of another circuit design.

Optimizing losses by circuit design

Let us look now at other types of converters. Using for example a forward converter instead of the flyback is a possibility. This structure will follow a different principle because of using a current storage choke (L).

$$V_S - V_{out} - V_L = 0$$

$$V_{out} - V_L$$

$$V_{in} \times \frac{N_{sec}}{N_{prim}} = V_{out} \times \frac{T}{t_{on}} = V_S$$

$$V_{in} = V_{out} \times \frac{N_{prim}}{N_{sec}} \times \frac{1}{DC}$$

Despite this, using a simple forward converter would bring along other disadvantages in terms of efficiency. Using a bridge topology will be another possible step of optimizing circuit design. This choice will also admit using a push-pull converter with extended performance range. Using the full bridge topology (figure 2), we have to take into account that four transistors are necessary to realize the circuit, but we do not have the negative effect caused by the reflected voltage that we saw for the flyback converter:

$$P_{loss,par} = 4 \times \frac{1}{2} \times 250pF \times (1000V)^2 \times \frac{1}{1.6\ ms} \approx 30\ W$$

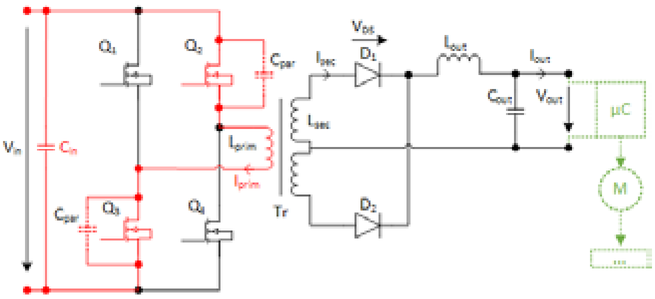

Figure 2: Full-bridge converter topology with midpoint circuit

Passing over now to a half bridge topology, where only two transistors are used, we will realize that the losses are only half as high as in the previous design:

$$P_{loss,par} = 2 \times \frac{1}{2} \times 250pF \times (1000V)^2 \times \frac{1}{16\ \mu s} \approx 15\ W$$

Nevertheless, referring to MVDC context, they still take a considerable part of the desired performance.

Following these examples, the power losses due to parasitic elements differ according to the topology in use, but they will in any case rise up to almost 6 -12% of the output power. As a result, reducing these parasitic elements has high priority in order to make the devices work in a more efficient way, but revising the circuit design is only one part of the answer. Another possibility would be reducing the switching frequency, but this comes along with limitation of the input voltage range and compromises in terms of component size. The same applies for optimizing the temperature stress, by adding elements as cooling fans and thicker aluminium heatsinks. In any case, for fulfilling the requirements in terms of reliability, EMC or weatherproofing, a large number of additional modules have to be added as well: It has to be emphasized that it is not possible to apply standard components. Nevertheless, many DC/DC converter producers that enter the field of renewable energy solutions did not yet face these issues because they had been specialized in low voltage applications where the problem is not as crucial as that. So a potential energy supplier would first have to develop its own system by assembling the necessary elements one by one, in a long and development-intensive process.

An all-in-one solution based on experience

In contrast, Grau Elektronik offers products that already include solutions to these specific MVDC requirements. Therefore, its developers refer to MVDC applications already realized in the field of railroad technology. As the producer looks back on twenty years of experience in the field, a large number of solutions for contact wire converters have been developed. Projects with similar context are, for example, converters installed at gated rail crossings. Depending on the surrounding area, they might be placed under extreme conditions as well, for example in weather-exposed locations or at altitudes. Hence, answers to reliability, EMC, vibration, climatic and heating issues are already implemented in the converter, so no need to add complementary elements as fuses, filters or heatsinks. Input/output separation with galvanic insulated current paths fit for safety and critical noise sensitive applications. Analog and digital current and voltage control loops decouple and provide microcontrollers, cooling fans, electric valves, contactors and sensors even in case of high fluctuations in supply voltage, load and temperature. Specialized for railroad applications, the existing converters are designed for 24/7 use and high MTBF, completely maintenance-free (figures 3 and 4). The nominal usage time of the

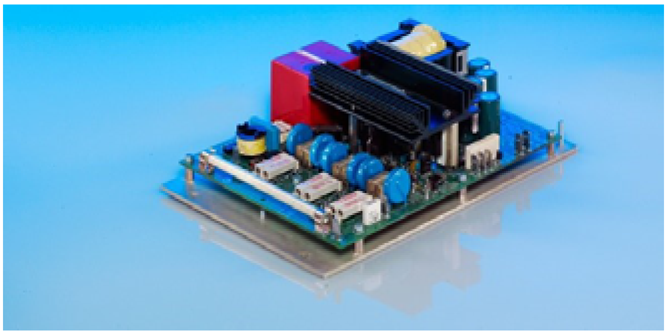

Figure 3: 250FDB 750 M24, a product developed for railroad technology

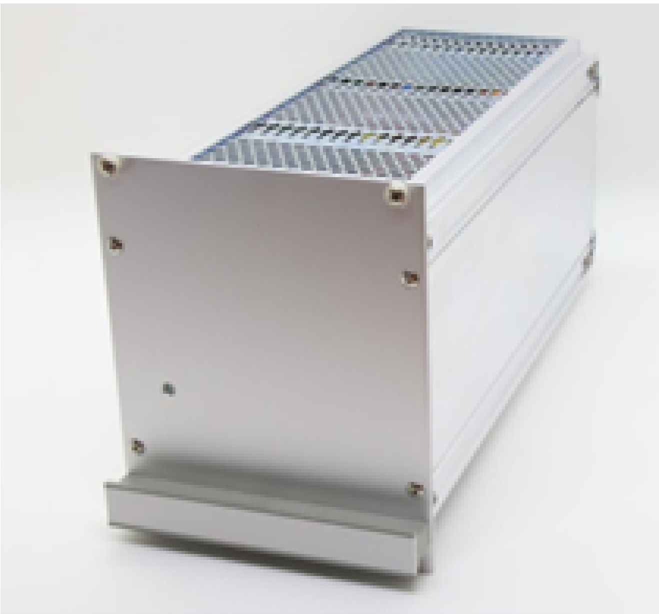

Figure 4: Sample product (250SWI 1000 M110)

converters is stated LT (LifeTime) for > 25 years referenced to average temperature Tamb = + 40°C. MTBF value is about λ < 800 fit referenced to nominal output power and Tamb = + 40°C. The converters are designed for three different input voltage ranges, as shown in the table below. The standard output voltage is 24V, others are available on request.

Power Range	Input Voltage Range	Output Voltage	Interfaces/ Signals
75W	$200V_{DC}$ – $1000V_{DC}$	24V, 48V, 110V	Powerfail, Enable, LEDs
	$800V_{DC}$ – $2250V_{DC}$		
150W	$250V_{DC}$ – $1000V_{DC}$		
	$800V_{DC}$ – $2250V_{DC}$		
250W	$250V_{DC}$ – $1000V_{DC}$		
	$1000V_{DC}$ – $2100V_{DC}$		
500W	$500V_{DC}$ – $1200V_{DC}$		

Tu: - 40°C ... + 70°C

It has to be mentioned that even input voltages up to 4000 V would be feasible. During a model project accompanied in the US, Grau Elektronik has already gained experience: Equipping a wind turbine by a device converting down an input voltage of 3000 V, the company has proofed its role as a pioneer in the field.

Summary and Outlook

As our grid's stability has highest priority, we realized how the use of DC/DC converters in renewable energy production and their storage applications puts heavy demands on the devices' reliability. Having considered the transformation of MVDC and the operation under extreme environmental conditions, we saw the rise of problems that are very different from those applying to conventional DC/DC converters, conceived for low voltages. We became aware of the fact how insulation, galvanic separation, EMC and thermal protection gained momentum. On the other hand, we discussed how increasing power losses threaten the efficiency of the process. Answers risk to be applied at the expense of component size and input voltage range. Standard components are far to be a solution to the requirements. Based on our experiences in railroad technology, we propose a device that includes all elements necessary for solving reliability, EMC, vibration, climatic and heating issues.

As higher voltages have to be used all over the process, it becomes clear that not only the primary energy production has to be rebuilt, but also the energy storage modules, as well as distribution grids and compensation systems. In conclusion, the optimization of the existing infrastructure will be an overall task that requires proofed knowledge in medium and high voltage applications.

www.grau-elektronik.de

How to Choose the Right Battery -Charger IC for Ultrasound Point-of-Care Products

In this article, I'll examine compact battery-charger integrated circuits (ICs) and solutions for ultrasound point-of-care products that are used by medical professionals to diagnose problems wherever a patient is receiving treatment.

By Jing Zou, Product Marketing Engineer for Battery Charger Products, Texas Instruments

Advancements in ultrasound imaging technology, along with rising demand for minimally invasive diagnostics and therapeutics, have made it possible to implement ultrasound applications for medical use. For example, employing ultrasound for remote patient monitoring has become increasingly

Figure 1: Point-of-care ultrasound devices (cart-based, notebook and handheld)

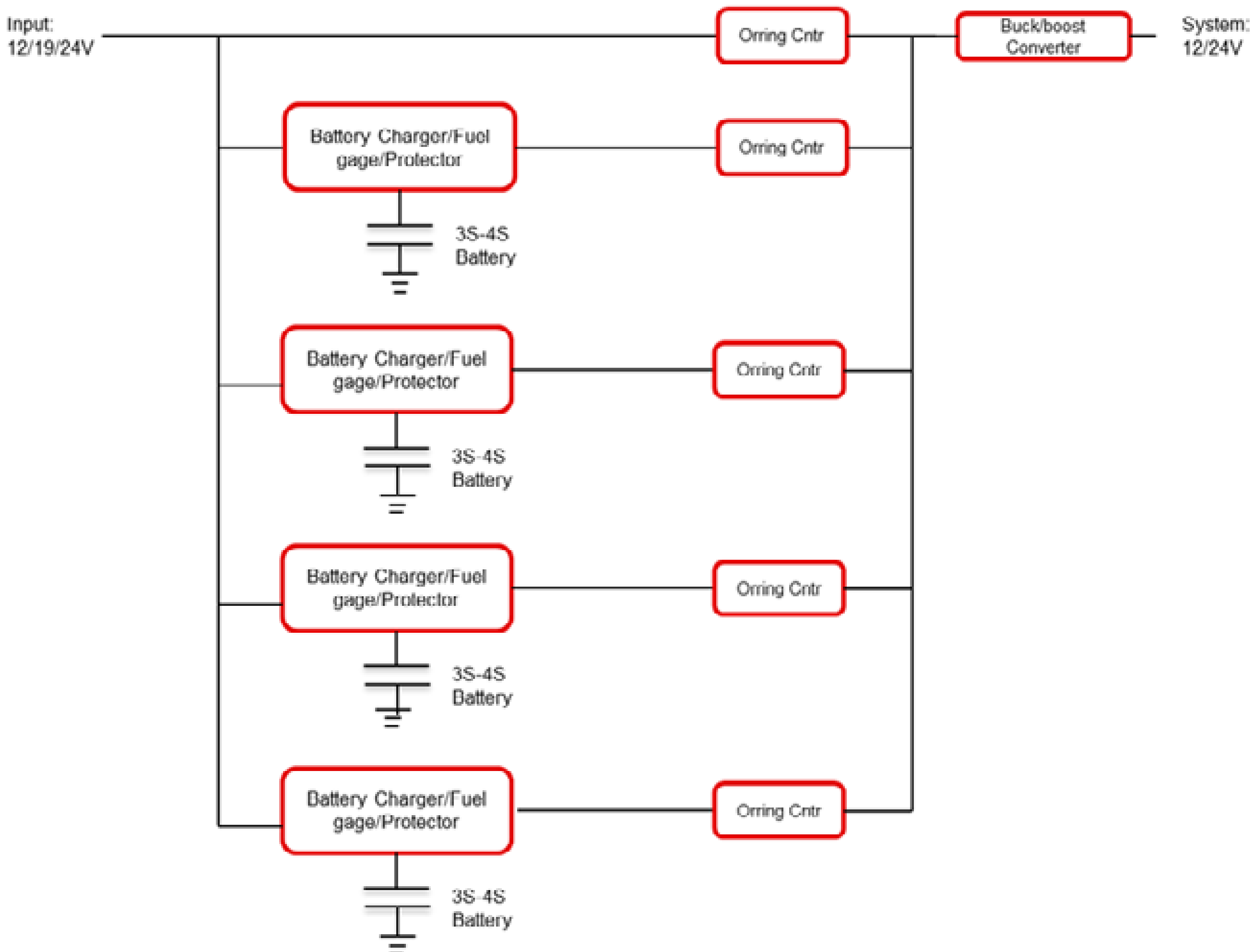

Figure 2: A simplified multi-battery pack battery-management system

popular given its cost-effective, safe and fast diagnostic capabilities. There is also demand for ultrasound devices to become more portable so that high-quality medical care can be consistently given anywhere from a hospital or doctor's office to someone's home or a remote village.

Types of point-of-care ultrasound devices and charging requirements

There are three major types of ultrasound devices: cart-based, notebook and handheld. System power consumption varies among the three. As a result, they need different battery configurations. As shown in Figure 1, a cart-based ultrasound machine is the most powerful of the three types. The maximum system current can be as high as 20 A at 12 V. The cart typically includes four individual battery packs connected in parallel to supply the system load sufficiently. Each battery pack is configured with four or more cells in series. Because of air traffic control regulations on lithium-based batteries, the capacitance of each battery pack cannot exceed 100 watt-hours. As a result, the four battery packs cannot be tied directly together. Each individual pack needs its own charging and discharging path, as illustrated in Figure 2.

Notebook-based devices also have a maximum battery capacity limitation of 100 watt-hours. System power consumption of an ultrasound notebook can go as high as 10 A at 12 V. Therefore, this type of machine typically includes two individual battery packs with separate charge and discharge paths.

The handheld smart probe is much smaller in size; it only collects and transmits data. Therefore, a single battery pack of one to two lithium-ion or lithium-polymer cells in series is sufficient to support operation. Unlike cart- or notebook-based ultrasound devices,

where the battery is used as backup power source, the battery in a smart probe is the main power source. Thus, fast charging with USB Type-C® Power Delivery, for example, is required for daily use.

Battery charger recommendations

Again, for cart-based and notebook devices, the battery serves as a backup and the line power is the main power source. Because of the high system current in these applications, you can use a direct power path where the system is powered by the input source directly. When the input source is removed, the direct power-path management automatically powers the system load from the battery.

TI's BQ24610 is a stand-alone battery-charge controller with direct power-path charging for up to six lithium-ion or lithium-polymer cells in series. The stand-alone feature makes charging parameters easily configurable through resistors.

For an ultrasound notebook, which can have multiple types of input sources that vary from 12 V to 24 V, the BQ25713 buck-boost charger can enable charging from different input sources without an additional DC/DC converter in front of the charger input. For the most compact ultrasound device, the smart probe, an integrated buck-boost charger like the BQ25790 offers a smaller solution size with high integration and chip-scale packaging. The device supports one to four cells in series and up to 5 A of battery current for fast charging. The input voltage range of 3.6 V to 24 V supports the full range for USB Type-C® Power Delivery. It also features a dual-input control that toggles between two power sources, such as wireless power or USB. Part of the same family of battery charger ICs, the BQ25792 comes in a quad flat no-lead (QFN) package to offer better thermal performance. For devices with one-cell configuration only, the BQ25892 or BQ25895 buck chargers can also be a good option, with a high charge-current capability up to 5 A. The D+/D- function detects standard USB ports and adjustable high-voltage adapters as input power sources.

As portability in ultrasound devices becomes more central when providing quality point-of-care patient diagnostics, you must optimize your battery designs. Different power levels require different battery design configurations, so it's important to understand your system and charging requirements in order to select the best battery charger integrated circuit.

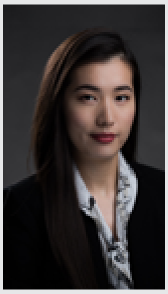

Jing Zou is a product marketing engineer for battery charger products at Texas Instruments. Previously, Jing has 6 years of experience as an application engineer of TI's battery charger products, where she supported a wide range of charger products including multi-cell switching chargers, linear chargers, and energy harvesting devices. She holds a bachelor's degree in electrical engineering from the University of Central Florida.

www.ti.com

Comparing Quasi-Resonant and Active Clamp Flyback Topologies for 65W Wall Charger Applications Using GaN Technology

Wall chargers using power GaN devices offer many advantages such as high-power density, higher efficiency and low operating temperatures compared to silicon-based solutions. This article discusses comparative results of ACF and QRF topology-based, 65W wall chargers using a GaN-based solution.

By Harshit Soni and Rajesh Ghosh, Tagore Technology Inc.

Introduction

With ever-increasing consumer demand for more compact, lightweight, low-cost power chargers for portable devices that can be quickly charged, efficient power conversion with higher switching frequencies are critical features for design engineers. Offering many advantages in terms of efficiency, power density and thermal performance compared to traditional silicon-based solutions, Gallium Nitride (GaN)-based devices are now being more widely adopted to solve the design challenges for applications such as cell phone wall chargers [1-6].

This article compares two 65 W, USB-PD wall charger prototypes based on two competing flyback topologies: quasi-resonant flyback (QRF) [1] and active clamp flyback (ACF) [2]. The QRF and ACF prototype chargers utilize a novel 650V, 360mΩ integrated GaN device, the TP44400NM that offers low output capacitance, low gate charge, and reduced parasitics. The wall chargers were tested to determine which approach presents the most elegant, energy efficient solution.

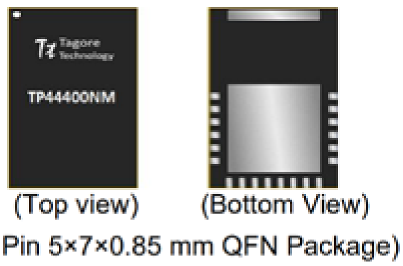

Figure 1: Tagore 360mΩ GaN Power IC, TP44400NM

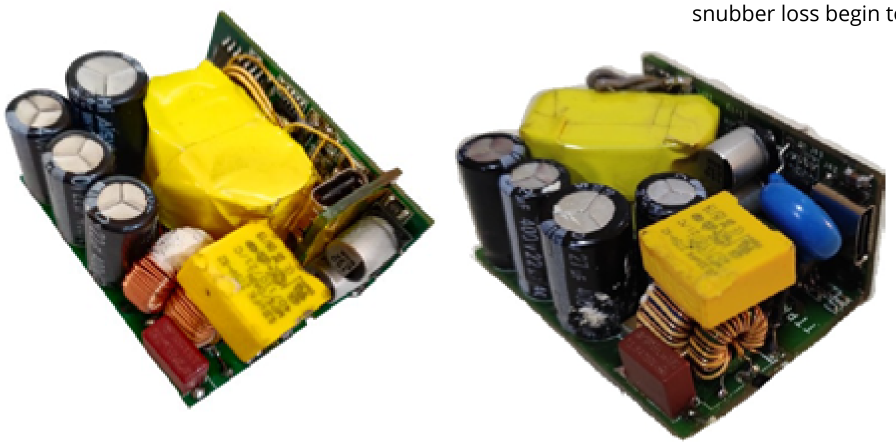

Figure 2: USB PD chargers with: ACF (left) and QRF (right) topologies.

GaN-based devices for USB-PD charger designs

Two 65W, USB-PD wall chargers based on QRF and ACF topologies **were designed using the TP44400NM 650V, 360mΩ integrated GaN** device (Figure 1). This GaN-based power IC with integrated driver, offered in a miniature QFN pack, offers extremely low conduction and switching losses to help meet stringent efficiency standards, delivers the required level of desired thermal performance for the application and enables a compact 30cc volume (corresponding to a power density of 35W/in3) design for both QRF and ACF- based charger solutions.

The two charger hardware prototypes based on the QRF and ACF topologies are shown in Figure 2. The ACF charger requires two GaN-based devices while the QRF charger requires only one GaN-based device.

The GaN-based ACF flyback converter [2] can clamp the primary switch voltage without any ringing and recycle the transformer leakage energy to the output without any snubber loss. This converter can be operated at a much higher switching frequency with the use of GaN devices while maintaining better efficiency and much higher power density than conventional Flyback chargers. One challenge in ACF design is the negative current needed for ZVS turn on of the main switch which increases the primary rms current leading to a higher conduction loss at the transformer and switches and core loss.

An alternative approach to increase conventional power charger efficiency is to adopt a GaN-based quasi-resonant flyback (QRF) topology [1] with a reduced valley switching loss at the primary side switch. Such designs are meant to be operated under 200kHz because at higher switching frequency the switching loss and the snubber loss begin to dominate.

Considering numerous design trade-offs in both chargers, such as switching frequency, system size versus frequency-related losses, the two chargers were designed to achieve the best possible performance.

Comparing ACF and QRF prototype chargers using an integrated GaN device

The ACF-based charger design utilizes two 360 mΩ GaN power ICs with integrated driver, the TP44400NM to keep the primary side conduction loss and core loss at a lower value by minimizing the -ve current requirement for ZVS. The QRF-based charger utilizes one GaN power IC with integrated driver.

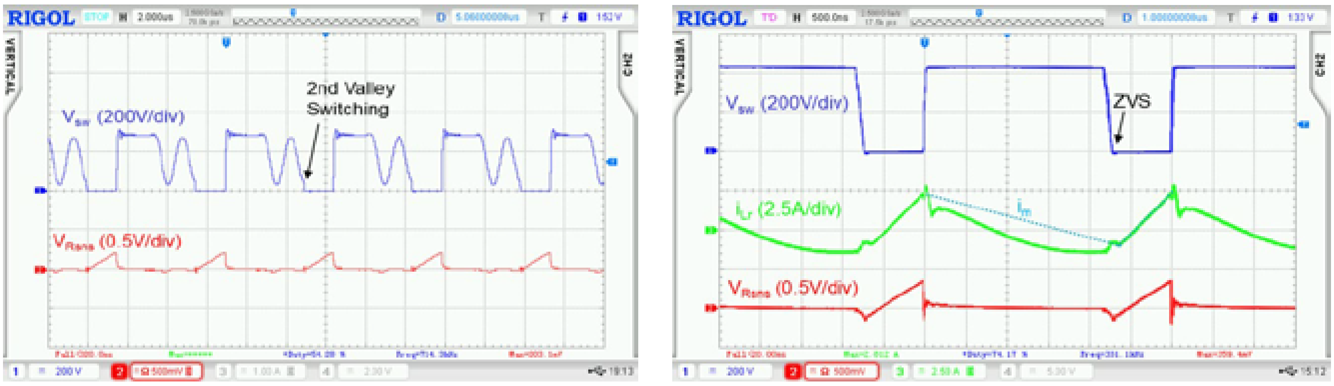

Figure 3: GaN drain switching waveforms of the QRF (left) and ACF (right) chargers.

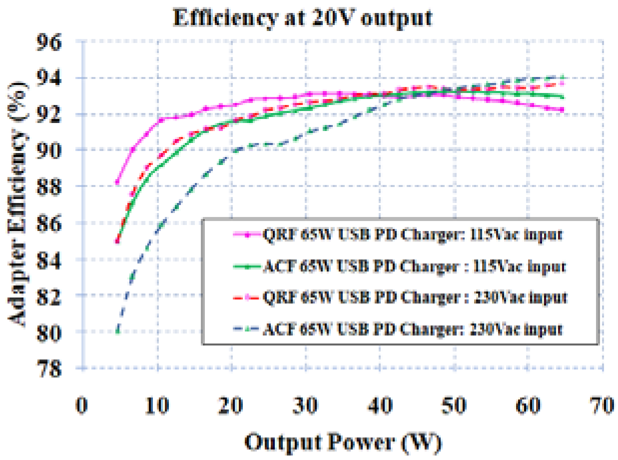

Figure 4: Comparative efficiencies of QRF and ACF chargers.

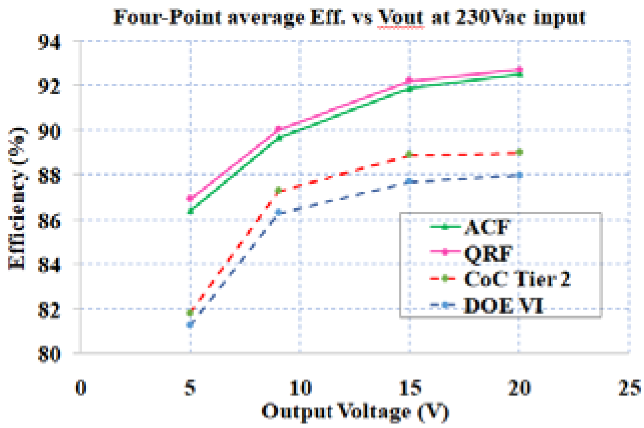

Figure 5: Comparative four-point efficiencies of QRF and ACF chargers.

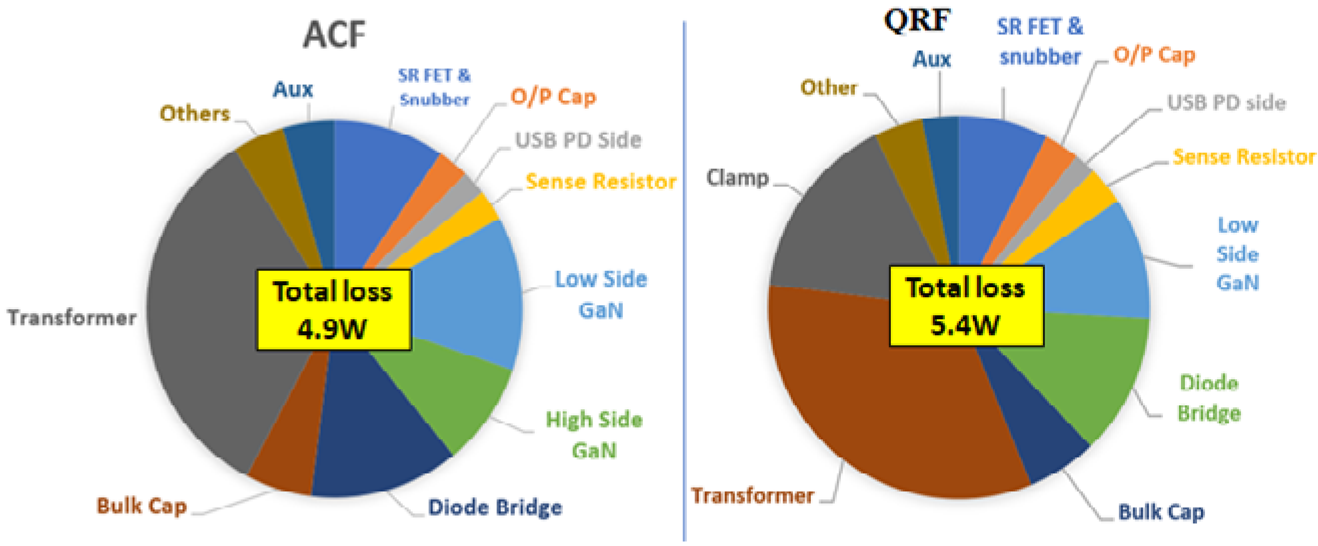

Figure 6: Full load loss distribution of ACF and QRF chargers.

Transformer design parameters such as Lm, n were selected so that the Fsw at 65 W load at 115Vac input line will be 100kHz and 300kHz for the QRF and ACF designs, respectively.

The GaN device drain switching waveforms of the two chargers at 115Vac input are shown in Figure 3. The QRF charger is shown to operate with valley switching turn on, while the ACF charger operates with ZVS switching turn. The comparative efficiencies, shown in Figure 4, indicate that the QRF is more efficient than the ACF prototype up to an output power of 45W, beyond which the efficiency of ACF charger dominates.

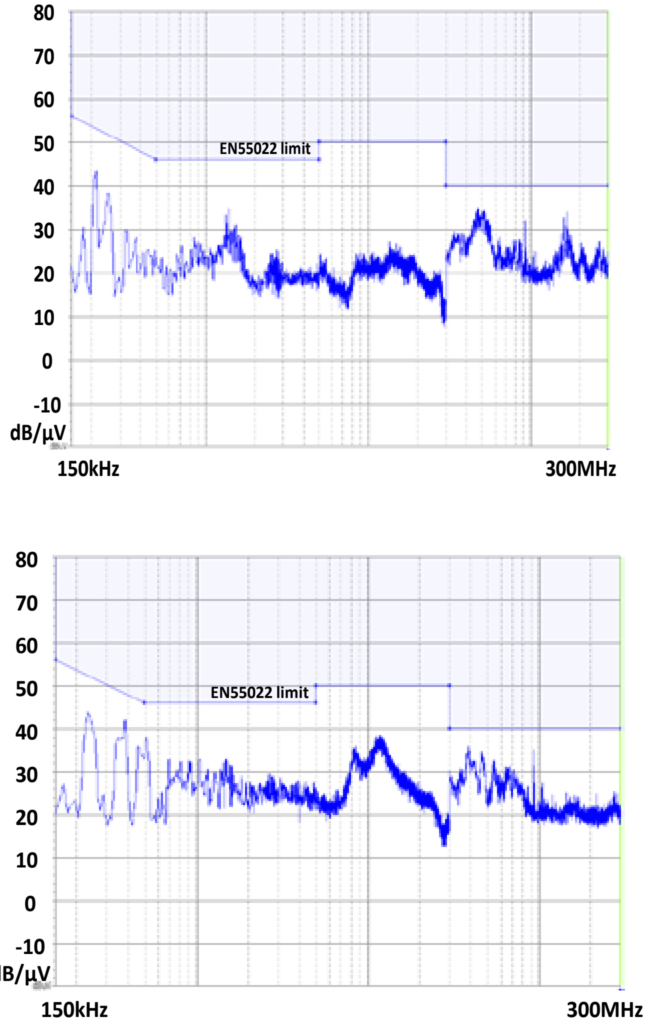

Figure 7: Conducted EMI test result of the ACF and QRF chargers.

USB-PD wall chargers need to meet stringent efficiency standards such as CoC Tie-2 and DoE Level VI. The four-point efficiencies of the two chargers, shown in Figure 5, closely follow each other, and both far exceed the limit lines specified by the above standards. The no load powers drawn by the QRF and ACF chargers are 45mW and 52mW, respectively. This helps comply with the no load power requirements specified in the previously referenced efficiency standards.

The distribution of power losses within various components of the chargers at full load is shown in Figure 6. It shows that the power loss in the GaN device is a small fraction of the total converter losses. Both the chargers have been tested thermally by putting them inside a closed box and running at full load for 30 minutes at room temperature. In both cases, the maximum GaN top plastic case temperatures were found to be less than 90°C.

The conducted EMI performances of the two chargers were tested for FCC Part 15 Class B EMI standard. Both chargers are seen to be passing the EMI at 220Vac input as shown in Figure 7.

Conclusion

Two USB-PD chargers using the TP44400NM 650V, 360mΩ integrated GaN device in a QFN package were analyzed.

While the ACF converter achieved ZVS at almost all load conditions at the cost of increased primary rms current, the core and winding loss at the coupled inductor also increased. This effect became prominent at light load where the efficiency drops as the switching frequency increased.

On the other hand, due to the valley switching and wastage of the leakage energy, the QRF converter had a 0.5-1% less full load efficiency than the ACF but a better light load efficiency profile for its moderate switching frequency and lower primary rms current leading to reduced transformer loss.

From the experimental efficiency data, it emerges that both topologies show similar average efficiency curves, resulting in both chargers meeting the CoC Tier-2 and DoE Level-VI energy standards, and the FCC Part 15 Class B EMI standard.

Consequently, it becomes the choice and requirements of the designer to choose between these two topologies for 65W adapter applications according to the sink load profile. On the other hand, the choice of the primary switching semiconductor device Rds(on) will depend on the maximum allowable temperature rise of the switching devices at full loading condition and at minimum rated input voltage in a closed case environment with the existing thermal design of the prototype.

The use of GaN-based technology for the main power switching device helps achieve higher power density and efficiency, and low operating temperature.

Based on this study, the QRF charger is found to be more efficient and has a simpler power train than the ACF charger up to 45W output power.

References

1. H. G. Mauromicale et al., “Si and GaN Devices in Quasi Resonant Flyback converters for Wall Charger Applications,” 2019 IEEE Energy Conversion Congress and Exposition (ECCE), Baltimore, MD, USA, 2019, pp. 3253-3258.
2. X. Huang, J. Feng, W. Du, F. C. Lee and Q. Li, “Design consideration of MHz active clamp flyback converter with GaN devices for low power adapter application,” 2016 IEEE Applied Power Electronics Conference and Exposition (APEC),Long Beach, CA, 2016, pp. 2334-2341.
3. J. Park et al., “Quasi-Resonant (QR) Controller with Adaptive Switching Frequency Reduction Scheme for Flyback Converter,” in IEEE Transactions on Industrial Electronics, vol. 63, no. 6, pp. 3571-3581, June 2016.
4. H. Onay, V. Suel and A. Hava, “An Comprehensive Loss Analysis of Quasi Resonant Flyback Converter for Design Purpose,” 2018 PCIM Asia, pp. 1-8.
5. S.L Jeng, M.T. Peng, C. Y. Hsu, W.H. Chieng and Jet P.H. Shu, “Quasi-Resonant Flyback DC/DC Converter Using GaN Power Transistors”, in World Electric Vehicle Journal, vol. 5, May 2012.
6. Pei-Hsin Liu, “Comparison of GaN- and Silicon FET-Based Active Clamp Flyback Converters”, Texas Instruments.

www.tagoretech.com

INCREASING POWER DENSITY FOR MOTOR DRIVES WITH SILICON CARBIDE

COMPACT DUAL INLINE PACKAGE

Footprint 58.7mm x 41.4mm

FEATURES

- Utilizes Silicon Carbon MOSFETs for superior performance
- High continuous output current – 30 A
- High supply voltage– 650 V maximum
- Fast switching frequency – 400 kHz
- Integrated with digitally controlled gate drive
- Under-voltage lock-out and active Miller clamping

TARGET APPLICATIONS

- BLDC Motor Drivers
- Variable Frequency Drives
- DC/AC Converters
- Power Inverters
- Test Equipment

APEX MICROTECHNOLOGY INC.
5980 N Shannon Road
Tucson, Arizona 85741 USA
T: +1.520.690.8600
F: +1.520.888.3329

SALES SUPPORT
Toll Free: +1.800.862.1032
eMail: custserv@apexanalog.com

TECHNICAL SUPPORT
Toll Free: +1.800.546.2739
eMail: Apex.Support@apexanalog.com

SA310: 3-PHASE SILICON CARBIDE MODULE

The SA310 is a fully integrated three-phase driver designed primarily to drive Brushless DC (BLDC) and Permanent Magnet Synchronous (PMSM) motors or DC/AC converters. The module uses Silicon Carbide MOSFET technology to improve efficiency over other devices in its class. Three independent half-bridges provide up to 80A peak output current under direct microcontroller or DSC control. The SA310 is built on a thermally conductive substrate that is electrically isolated to provide the most versatility and ease in heatsinking.

The amplifier protection features include under-voltage lockout (UVLO) function and active Miller clamping to reduce switching noise and improve reliability. Also included in the module are Silicon Carbide Schottky Barrier free-wheeling diodes to protect the body diode of each MOSFET. No external output protection diodes are required. The SA310's integrated gate drivers provide transformer isolation between the inputs and high-voltage outputs.

TYPICAL APPLICATION

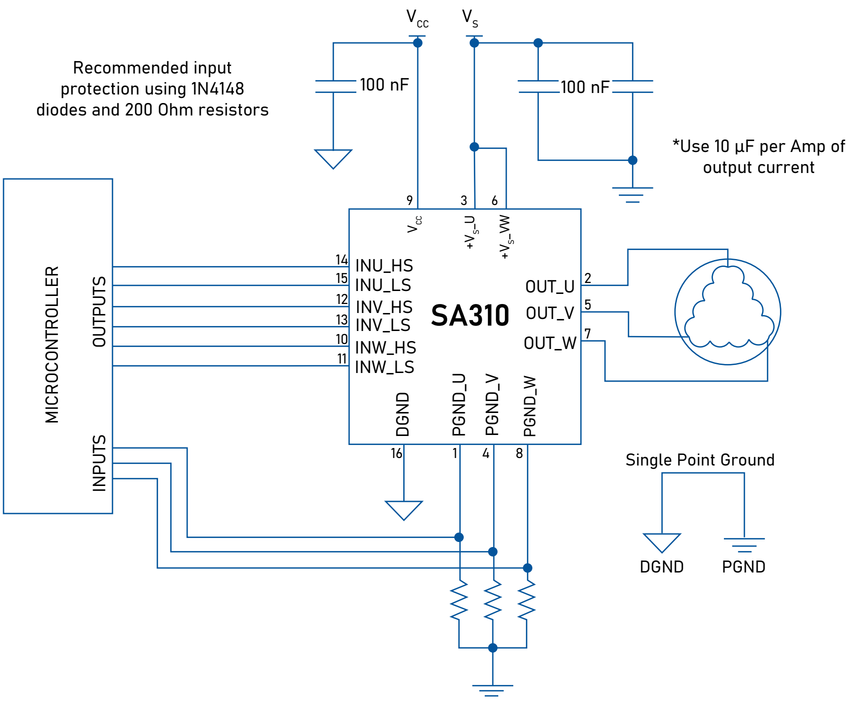

APEXANALOG.COM/PRODUCTS/SA310

ISO9001

Energy Storage Using Supercapacitors: How Big Is Big Enough?

In a power backup or holdup system, the energy storage medium can make up a significant percentage of the total bill of materials (BOM) cost, and often occupies the most volume. The key to optimizing a solution is careful selection of components so that holdup times are met, but the system is not overdesigned.

By Markus Holtkamp, Field Applications Engineer, and Gabino Alonso, Director of Strategic Marketing, Analog Devices

That is, one must calculate the energy storage required to meet holdup/backup time requirements over the lifetime of the application, without excessive margin. This article presents a strategy for choosing a supercapacitor and a backup controller for a given holdup time and power, considering the vagaries of supercapacitors over their lifetimes.

Electrostatic double-layer capacitors (EDLC), or supercapacitors (supercaps), are effective energy storage devices that bridge the functionality gap between larger and heavier battery-based systems and bulk capacitors. Supercaps can tolerate significantly more rapid charge and discharge cycles than rechargeable batteries can. This makes supercaps better than batteries for short-term energy storage in relatively low energy backup power systems, short duration charging, buffer peak load currents, and energy recovery systems (see Table 1). There are existing battery-supercap hybrid systems, where the high current and short duration power capabilities of supercapacitors complement the long duration, compact energy storage capabilities of batteries.

Feature	Supercapacitors	Li-Ion Battery
Charge/Discharge Time	<1 s to >10 s	30 min to 600 min
Termination/Overcharge	—	Yes
Charge/Discharge Efficiency	85% to 98%	70% to 85%
Cycle Life	100,000+	500+
Min to Max Cell Voltage (V)	0 to 2.3*	3 to 4.2
Specific Energy (Wh/kg)	1 to 5	100 to 240
Specific Power (W/kg)	10,000+	1000 to 3000
Temperature (°C)	–40°C to +45°C*	0°C to +45°C charge*
Self-Discharge Rate	High	Low
Intrinsic Safety	High	Low

*To preserve reasonable lifetime

Table 1: Comparison Between EDLC and Li-Ion Batteries

It is important to note that higher temperatures and higher cell voltages in supercaps decrease a supercap's lifetime. It is important to ensure that the cell voltages do not exceed temperature and

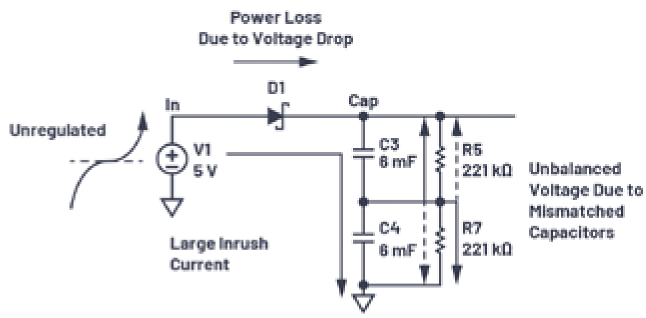

Figure 1: An example of an overly simple design resulting in a risky supercap charging scheme.

	LTC3110	LTC4041	LTC3350	LTC3351	LTC3355
V_{IN} (V)	1.8 to 5.25	2.9 to 5.5 (60 V OVP)	4.5 to 35	4.5 to 35	3 to 20
Charger ($V_{IN} \rightarrow V_{CAP}$)	2 A buck-boost	2.5 A buck	10+ A buck controller	10+ A buck controller	1 A buck
Number of Cells	2	1 to 2	1 to 4*	1 to 4*	1
Cell Balancing	Yes	Yes	Yes	Yes	—
V_{CAP} (V)	0.1 to 5.5	0.8 to 5.4	1.2 to 20	1.2 to 20	0.5 to 5
DC-to-DC ($V_{CAP} \rightarrow V_{OUT}$)	2 A buck-boost	2.5 A boost	10+ A boost controller	10+ A boost controller	5 A boost
V_{OUT} Range (V)	1.8 to 5.25	2.7 to 5.5	4.5 to 35	4.5 to 35	2.7 to 5
PowerPath	Internal FET	External FET	External FET	External FET	Separate boost
Inrush Current Limiting	—	—	—	Yes	—
Systems Monitoring	—	PWR fail, PG	V, I, cap, ESR	V, I, cap, ESR	VIN, VOUT, VCAP
Package	24-lead TSSOP, 24-lead QFN	4 mm × 5 mm, 24-lead QFN	5 mm × 7 mm, 38-lead QFN	5 mm × 7 mm, 38-lead QFN	4 mm × 4 mm, 20-lead QFN

*Can be configured for more than four capacitors

Table 2: Feature Summary of Integrated Supercap Charger Solutions

voltage ratings, and that these parameters remain within desired operation levels in applications where supercapacitors are stacked or when the input voltage is not well regulated (see Figure 1).

It can be difficult to achieve a robust and efficient solution using discrete components. In contrast, integrated supercap charger/ backup controller solutions are easy to use and typically provide most or all of these features:

- A well-regulated cell voltage regardless of the input voltage variations
- Active voltage balancing of individual stacked cells to ensure the voltage is matched during all operating conditions regardless of mismatches between cells
- Low conduction losses and low dropout voltage on cell voltage to ensure the system gets the maximum amount of energy for a given supercapacitor
- Inrush current limiting for live insertion of boards
- Communication with a host controller

Selecting the Right Integrated Solution
Analog Devices has an extensive lineup of integrated solutions that incorporate all necessary circuitry to cover the fundamentals of your backup system in a single IC. Table 2 summarizes the features of some Analog Devices supercap chargers.

For applications with 3.3 V or 5 V supply rails, consider:

- The LTC3110: a 2 A bidirectional buck-boost dc-to-dc regulator and charger/balancer
- The LTC4041: a 2.5 A supercapacitor backup power manager

For applications with 12 V or 24 V supply rails, or if you require backup power beyond 10 W, consider:

- The LTC3350: a high current supercapacitor backup controller and system monitor
- The LTC3351: a hot swappable supercapacitor charger, backup controller, and system monitor

If your system requires a main buck regulator for 3.3 V or 5 V rails with a built-in boost converter for backup using a single supercapacitor or other energy source for temporary backup or ride-through, you should consider:

- The LTC3355: a 20 V, 1 A buck dc-to-dc with integrated supercapacitor charger and backup regulator

Analog Devices also has many other constant current/constant voltage (CC/CV) solutions that can be used to charge a single supercapacitor, electrolytic capacitor, Li-Ion battery, or NiMH battery.

Calculating Holdup or Backup Time
When designing a supercapacitor energy storage solution, how big is big enough? To limit the scope of this analysis, let's focus on the classic holdup/backup applications used in high end consumer electronics, portable industrial equipment, energy metering, and military applications.

A good analogy for this design task would be a hiker who wants to determine how much water to carry on a day-long hike. Less water at the start certainly makes going uphill easy, but he may run out of water too early, especially for a difficult hike. On the other hand, a hiker carrying a large bottle of water must endure the additional weight, but will likely stay hydrated throughout the duration of the trip. The hiker may also have to take weather into account: more water on a hot day, less when cool.

Choosing a supercapacitor is very similar; holdup duration and load are important, as is ambient temperature. Furthermore, one must take into account the lifetime degradation of the nominal capacitance and the inherent ESR of the supercapacitor. Generally, the definition of the end-of-life (EOL) parameters for supercapacitors are:

- Specified (initial) capacitance has decreased to 70% of nominal.
- ESR has doubled from the specified initial value.

These two parameters are important to the following calculations.

To size your power components, it is important to understand your holdup/ backup load specifications. In the case of a power failure, for example, the system might disable noncritical loads, so that energy can be shuttled to key circuits, such as those that save data from volatile to nonvolatile memory.

Power failures come in many forms, but generally backup/holdup power must enable the system to gracefully shutdown in the face of a persistent failure or continue to operate through a transitory power failure.

In either of these cases, the component sizing must be worked out based on the sum of the loads that requires support during backup/holdup and the time those loads must be supported.

The amount of energy that is required to holdup or backup the system:

$$Energy_{Required} = \frac{1}{Efficiency} \times Power \times Time \qquad (1)$$

The stored energy in a capacitor:

$$Energy_{Stored} = \frac{1}{2} C\, V_{Capacitor}^2 \qquad (2)$$

Common sense design dictates that the energy stored in the capacitor must be greater than what is required for holdup or backup:

$$Energy_{Stored} > Energy_{Required} \qquad (3)$$

This approximates the size of the capacitor, but is not sufficient to determine the size for a truly robust system. Key details must be determined, such as the various sources of energy loss, which ultimately translate to greater required capacitance. Energy losses fall into two categories: those due to dc-to-dc converter efficiency, and those from the capacitor itself.

The efficiency of the dc-to-dc converter must be known for the condition where the supercapacitor is powering the load during holdup or backup. Efficiency depends on the duty cycle (line and load) conditions and can be obtained from the controller data sheet. The devices noted in Table 2 above have a peak efficiency of 85% to 95%, which can vary over the load current and duty cycle during the holdup or backup.

Supercapacitor energy loss amounts to the energy we cannot extract from the supercapacitor. This loss is determined by the minimum input operating voltage of the dc-to-dc converter. This is de-

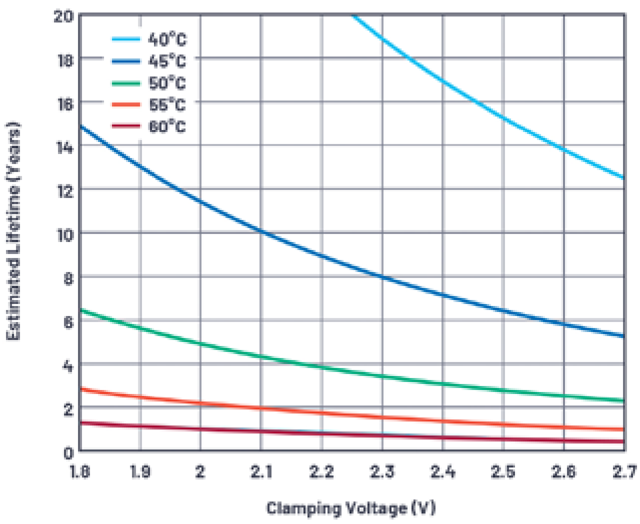

Figure 2: A diagram of lifetime vs. clamping voltage, using temperature as the key parameter.

pendent on the topology of the dc-to-dc converter and is called the dropout voltage. This is an important parameter to consider when comparing integrated solutions.

Taking the earlier calculation for the energy of a capacitor and subtracting the energy unavailable below $V_{Dropout}$ results in:

What about $V_{Capacitor}$? It seems obvious that setting $V_{Capacitor}$ to near its max rating would increase the stored energy, but this strategy has serious drawbacks. Often, supercapacitors have an absolute maximum voltage rating of 2.7 V, but the typical value is 2.5 V or less. This is due to the lifetime consideration of the application and its specified ambient temperature of operation (see Figure 2). By using a higher $V_{Capacitor}$ in a higher ambient temperature, the lifetime of the supercapacitor is degraded. For robust applications requiring a long operating lifetime or operation at relatively high ambient temperatures, a lower $V_{Capacitor}$ is best. Individual supercapacitor suppliers usually supply characteristic curves for estimated lifetime based on clamping voltage and temperature.

Maximum Power Transfer Theorem

The third effect that must be taken into consideration is not so obvious: the maximum power transfer theorem. To obtain maximum external power from a supercapacitor source with an equivalent series resistance (see Figure 3), the resistance of the load must equal the resistance of the source. This article uses the words out, backup, or load interchangeably as all three mean the same thing in this case.

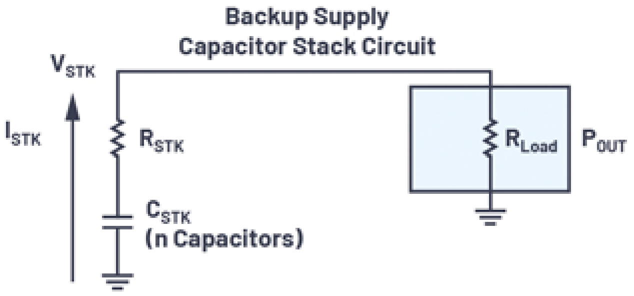

Figure 3: Power delivery from a capacitor stack with series resistance.

If we take the diagram in Figure 3 as a Thevenin equivalent circuit, we can easily calculate the amount of power dissipated across the load via:

$$P_{OUT} = V_{STK}^2 \frac{R_{Load}}{(R_{STK} + R_{Load})^2} \quad (5)$$

$$P_{OUT} = (I_{STK} R_{STK})^2 \frac{R_{Load}}{(R_{STK} + R_{Load})^2} \quad (6)$$

To find the maximum power transfer, we can take the derivative of the previous equation and then solve for the condition when it is zero. This is the case when $R_{STK} = R_{LOAD}$.

Allowing $R_{STK} = R_{LOAD}$, we can obtain:

$$P_{OUT(MAX)} = \frac{V_{STK}^2}{4R_{STK}} \quad (7)$$

This can also be approached intuitively. That is, if the resistance of the load is greater than the source resistance, the load power is reduced, since the total circuit resistance goes up. Likewise, if load resistance is lower than source resistance, then most of the power is dissipated in the source due to a lower total resistance; similarly, the amount dissipated in the load is reduced. Therefore, deliverable power is maximized when source and load impedance are matched for a given capacitance voltage and a given stack resistance (ESR of the supercapacitors).

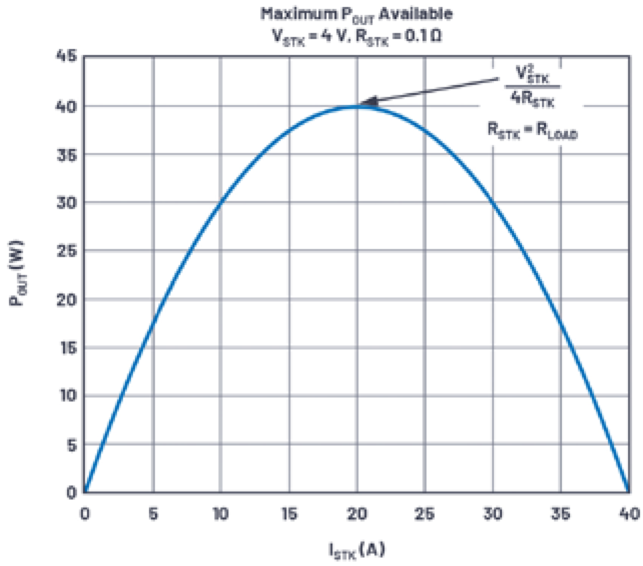

Figure 4: Curve of available power vs. stack current.

There are implications with regard to the usable energy in a design. As the ESRs of the stacked supercapacitors are fixed, then the only value that varies during backup operation is the stack voltage and, of course, the stack current.

To satisfy the backup load requirements, as the stack voltage decreases, the required current to support the load increases. Unfortunately, increasing currents beyond the defined optimum level reduces the available backup power, as it increases the losses in the ESR of the supercapacitors. If this effect occurs before the dc-to-dc converter reaches its minimum input voltage, it translates into additional loss of usable energy.

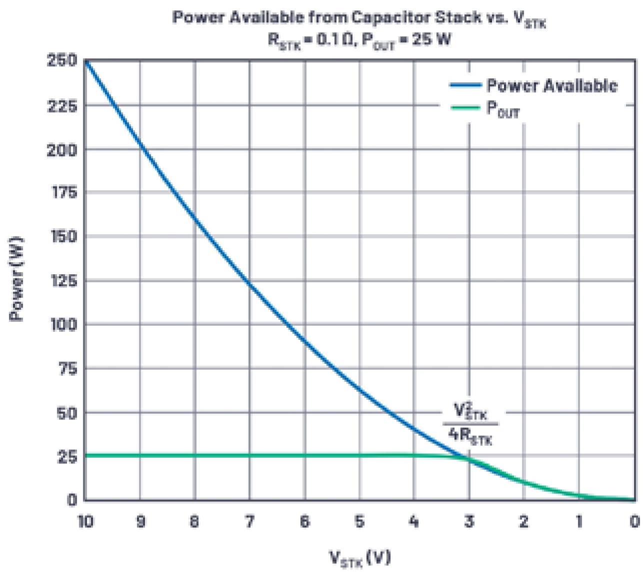

Figure 5: This diagram shows the derivation of minimum V_{IN} required for certain output power.

Figure 5 shows the available power as a function of VSTK, assuming an optimal resistance matching to the load, and the graph of 25 W of backup power. This graph can also be viewed as a unitless time base: as the supercapacitors satisfy the 25 W of required backup power, the stack voltage decreases as it discharges into the load. At 3 V, there is an inflection point at which the load current is beyond the optimum level, decreasing the available backup power for the load. This is the maximum deliverable power point of the system, and at this point, losses in the ESR of the supercapacitors increase. In this example, 3 V is significantly higher than the dropout voltage of the dc-to-dc converter, so unusable energy is due entirely to the supercapacitor, leaving the regulator underutilized. Ideally, the supercap reaches the dropout voltage, so the system's ability to provide power is maximized.

Taking the earlier equation for PBACKUP, we can solve for VSTK(MIN). Likewise, we can also take into consideration the efficiency of the boost converter and add it to this equation:

$$V_{STK(MIN)} = \sqrt{4R_{STK}P_{Backup}} \tag{8}$$

$$Boost\ Operation:\ V_{STK(MIN)} = \sqrt{\frac{4R_{STK}P_{Backup}}{\eta}} \tag{9}$$

With this lower limit $V_{STK(MIN)}$, we can establish a capacitor utilization ratio αB, which is derived from the maximum and minimum cell voltage:

$$\alpha_B = \frac{V^2_{STK(MAX)} - V^2_{STK(MIN)}}{V^2_{STK(MAX)}} \tag{10}$$

Not only is the supercapacitor capacitance vital for determining the backup time, but the ESR of the capacitor is as well. The supercapacitor's ESR determines how much of the stack voltage can be used for the backup load, also known as utilization ratio.

As the backup process is a dynamic process in terms of input voltage, output current, and duty cycle, the complete formula for required stack capacitance is not as simple as the earlier versions. It can be shown that the final formula is:

$$C_{SC} \geq \frac{2P_{Backup}t_{Backup}}{n\,\eta\,V^2_{STK(MAX)}\left[\frac{\alpha_B + \sqrt{\alpha_B}}{2} - \frac{1-\alpha_B}{2}\ln\left(\frac{1+\sqrt{\alpha_B}}{\sqrt{1-\alpha_B}}\right)\right]} \tag{11}$$

where η = Efficiency of the dc-to-dc converter.

The concepts and calculations to this point can be translated into a supercap backup system design methodology:

- Determine the backup requirements for P_{Backup} and t_{Backup}.
- Determine the maximum cell voltage, $V_{STK(MAX)}$, for desired lifetime of capacitor.
- Choose the number of capacitors in the stack (n).
- Choose a desired utilization ratio, αB for the supercapacitor (for example, 80% to 90%).
- Solve for capacitance C_{SC}:

$$C_{SC} \geq \frac{2P_{Backup}t_{Backup}}{n\,\eta\,V^2_{STK(MAX)}\left[\frac{\alpha_B + \sqrt{\alpha_B}}{2} - \frac{1-\alpha_B}{2}\ln\left(\frac{1+\sqrt{\alpha_B}}{\sqrt{1-\alpha_B}}\right)\right]} \tag{12}$$

Find a supercapacitor with sufficient C_{SC} and check if the minimum R_{SC} formula is fulfilled:

$$R_{SC} \leq \frac{\eta\,(1-\alpha_B)\,n\,V_{STK(MAX)}}{4P_{Backup}} \tag{13}$$

If a suitable capacitor is not available, iterate by choosing more capacitance, a higher cell voltage, more capacitors in the stack, or a lower utilization ratio.

Taking Supercapacitor End of Life into Account

For a system that must reach a certain lifetime, the previously described methodology must be modified with EOL values, generally 70% of CNOM and 200% of ESRNOM. This complicates the math, but existing spreadsheet tools are available on product webpages for most ADI supercapacitor managers.

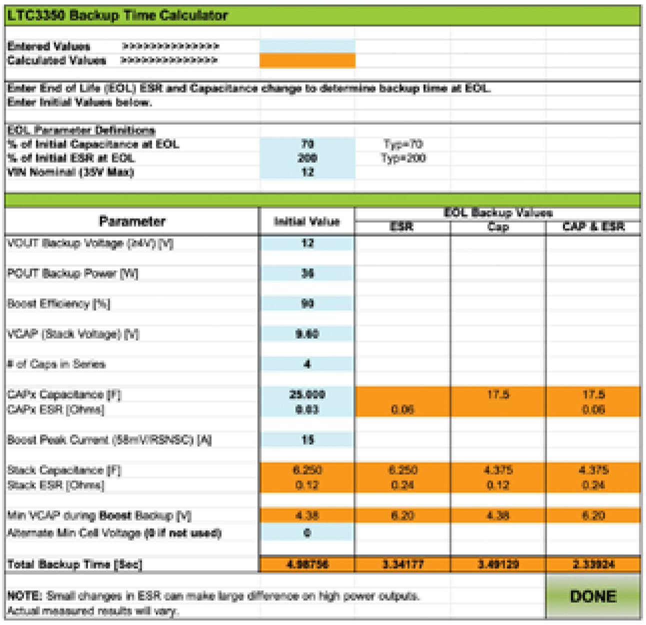

LTC3350 Backup Time Calculator				
Entered Values >>>>>>>>>>>>>>				
Calculated Values >>>>>>>>>>>>>>				
Enter End of Life (EOL) ESR and Capacitance change to determine backup time at EOL.				
Enter Initial Values below.				
EOL Parameter Definitions				
% of Initial Capacitance at EOL	70	Typ=70		
% of Initial ESR at EOL	200	Typ=200		
VIN Nominal (35V Max)	12			
		EOL Backup Values		
Parameter	Initial Value	ESR	Cap	CAP & ESR
VOUT Backup Voltage (≥4V) [V]	12			
POUT Backup Power [W]	36			
Boost Efficiency [%]	90			
VCAP (Stack Voltage) [V]	9.60			
# of Caps in Series	4			
CAPx Capacitance [F]	25.000		17.5	17.5
CAPx ESR [Ohms]	0.03	0.06		0.06
Boost Peak Current (58mV/RSNSC) [A]	15			
Stack Capacitance [F]	6.250	6.250	4.375	4.375
Stack ESR [Ohms]	0.12	0.24	0.12	0.24
Min VCAP during Boost Backup [V]	4.38	6.20	4.38	6.20
Alternate Min Cell Voltage (0 if not used)	0			
Total Backup Time [Sec]	4.98756	3.34177	3.49129	2.33924
NOTE: Small changes in ESR can make large difference on high power outputs. Actual measured results will vary.				DONE

Figure 6: LTC3350/LTC3351 calculation for a 36 W, 4 s holdup system with 25 F capacitance.

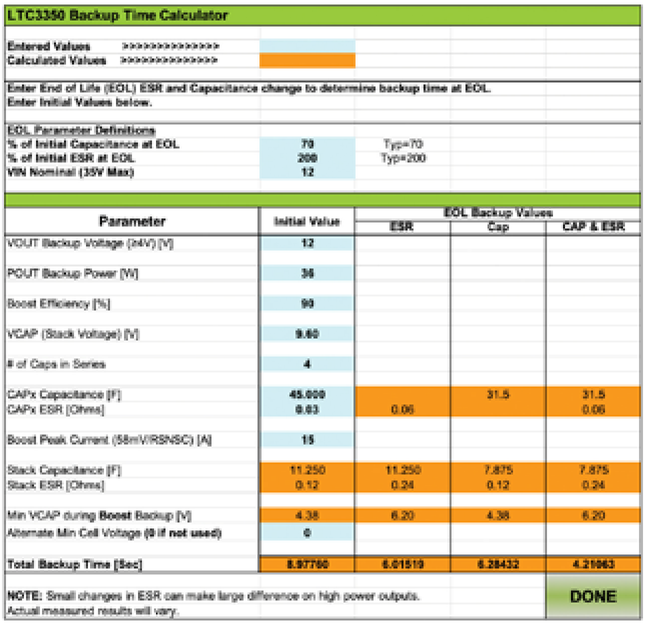

LTC3350 Backup Time Calculator				
Entered Values >>>>>>>>>>>>>>				
Calculated Values >>>>>>>>>>>>>>				
Enter End of Life (EOL) ESR and Capacitance change to determine backup time at EOL.				
Enter Initial Values below.				
EOL Parameter Definitions				
% of Initial Capacitance at EOL	70	Typ=70		
% of Initial ESR at EOL	200	Typ=200		
VIN Nominal (35V Max)	12			
		EOL Backup Values		
Parameter	Initial Value	ESR	Cap	CAP & ESR
VOUT Backup Voltage (≥4V) [V]	12			
POUT Backup Power [W]	36			
Boost Efficiency [%]	90			
VCAP (Stack Voltage) [V]	9.60			
# of Caps in Series	4			
CAPx Capacitance [F]	45.000		31.5	31.5
CAPx ESR [Ohms]	0.03	0.06		0.06
Boost Peak Current (58mV/RSNSC) [A]	15			
Stack Capacitance [F]	11.250	11.250	7.875	7.875
Stack ESR [Ohms]	0.12	0.24	0.12	0.24
Min VCAP during Boost Backup [V]	4.38	6.20	4.38	6.20
Alternate Min Cell Voltage (0 if not used)	0			
Total Backup Time [Sec]	8.97760	6.01519	6.28432	4.21063
NOTE: Small changes in ESR can make large difference on high power outputs. Actual measured results will vary.				DONE

Figure 7: LTC3350/ LTC3351 calculation with 45 F capacitance.

Let's use a simplified methodology with example using the LTC3350:

- Required backup power is 36 W for a duration of four seconds.
- $V_{CELL(MAX)}$ is set to 2.4 V for longer lifetime/higher ambient temperature.
- Four capacitors are series stacked.
- DC-to-DC efficiency (η) is 90%.

Using an initial guess of 25 F capacitance, the spreadsheet tool provides the result shown in Figure 6.

Based on the initial guess of 25 F capacitance, we obtain the required four seconds of backup time (with an additional 25% margin) using nominal values. However, if we consider the EOL values of ESR and capacitance, our backup time drops to almost half. To obtain four seconds with the EOL values of the capacitors, we must modify at least one of our input parameters. Since most of them are fixed, the capacitance is the most convenient parameter to increase.

- Increasing the capacitance to 45 F, the spreadsheet tool provides the result shown in Figure 7.

The necessary increase toward 45 F seems large since the nominal values provide a comfortable nine seconds of backup. However, with the addition of CAP_{EOL} and ESR_{EOL}, and the resulting minimum stack voltage of 6.2 V, there is a sharp degradation to half of the backup time at EOL. Nevertheless, this meets our four second requirement for holdup time with an additional 5% margin.

Additional Supercap Manager Features

The LTC3350 and LTC3351 offer additional telemetry features via an integrated ADC. These parts can measure the system voltages, currents, capacitance, and ESR of the supercapacitor stack. Capacitance and ESR measurements are performed with minimal impact to the system while it is online. Device configuration and measurements are communicated via I2C/SMBus. This enables the system processor to monitor important parameters over the life of the application, ensuring that available backup power meets the system requirements.

The LTC3350's and the LTC3351's capability to measure the capacitance and ESR of the supercapacitor stack in real time enables the user to reduce the clamp voltage when the capacitors are new and easily meet the backup requirements. The processor receiving the telemetry data can be programmed to implement the previously shown calculations. This would enable the system to calculate, on-the-fly, the minimum necessary clamp voltage to satisfy the backup time, considering real-time capacitance and ESR. This algorithm would further enhance the lifetime of the supercapacitor backup system, because, as shown in Figure 2, at elevated temperatures, the lifetime of the supercapacitors can be significantly increased by even a small decrease in the clamp voltage.

Lastly, the LTC3351 features a hot swap controller function for protection purpose. The hot swap controller uses back-to-back N-channel MOSFETs to provide foldback current limiting, which reduces inrush current and short circuit protection in highly available applications.

Conclusion

Calculating the capacitance values required to meet backup specifications can be approached as a simple power needed, power stored problem by using the basics of energy transfer at nominal values. Unfortunately, this simple approach falls short when you consider the impact of maximum power transfer, a capacitor's EOL capacitance, and ESR. These factors greatly impact the available energy in a system over its lifetime. Using ADI's integrated supercapacitor solutions and a number of available backup time calculation tools, analog engineers should have the confidence to design and build reliable supercapacitor backup/holdup solutions that meet design requirements over an application's lifetime with minimum impact on cost.

www.analog.com

About the Authors:

Markus Holtkamp received his degree from the University of Bochum in 1993. He joined Linear Technology (now part of Analog Devices) in October 2010 as a field applications engineer (FAE) to provide technical support to customers in Central Europe. Markus' experience includes 14 years as an IC designer (high speed and mixed-signal ASICs) in a German design house and 3.5 years at Arrow Electronics as an analog FAE. He is married with two children and is an avid sports participant.

Gabino Alonso is currently the director of strategic marketing for the Power by Linear™ Group. Prior to joining ADI, Gabino held various positions in marketing, engineering, operations, and education at Linear Technology, Texas Instruments, and California Polytechnic State University. He holds a Master of Science degree in electrical and computer engineering from University of California, Santa Barbara.

9th ECPE SiC & GaN User Forum

"Potential of Wide Bandgap Semiconductors in Power Electronic Applications"
Munich/virtual (hybrid), 30 June - 01 July 2021

The biannual ECPE Wide Bandgap User Forum is dedicated to report and discuss state of the art and prospects of SiC and GaN devices in power electronic systems.

By Andreas Lindemann, Otto-von-Guericke-Universität Magdeburg, Chair for Power Electronics

Overview

Major progress has been achieved in the meantime: Today SiC transistors and diodes are available within a wide voltage range and from various manufacturers; they are used in a variety of products. Application-specific aspects gain importance, such as qualification when exposed to demanding mission profiles in electric vehicles. Of course research and development to optimise the devices continuously and extend their operational range continue in parallel. In a similar way GaN power transistors have matured and penetrated various applications while research and development are ongoing as well. In addition, R&D is dedicated to further devices based on other materials.

This year's ECPE wide bandgap user forum was special since it had been postponed due to the pandemic situation, this way permitting it to be carried out as one of the first hybrid events in the area of power electronics this year, with some of the participants taking part on site and others remotely; the exchange which became possible again this way was highly appreciated.

State of the Art and Trends

From application point of view, 650V GaN HEMTs are competing with charge compensated silicon MOSFETs in particular in power supplies; in addition optimised 650V SiC MOSFETs might replace the formers as well. This permits to increase the efficiency or the power density of the respective converters which are usually single phase off-grid versions with power factor correction, or DC-DC converters such as in the on-board grid of electric vehicles. Switching frequency may reach up to considerable 1MHz in this voltage class. Similar aims — optimisation of efficiency or power density — can be realised with SiC MOSFETs for 1200V or higher blocking voltages in converters connected to the three-phase grid, e. g. being part of wind generator systems. In this voltage range solutions with silicon transistors and SiC diodes may in addition still permit an optimisation compared to converters with silicon devices only. The usage of SiC and GaN devices of course requires that they are qualified, reach an appropriate reliability under consideration of the mission profile and also provide enough ruggedness. Major progress in device development, standardisation and qualification has been reported in this respect as well as ongoing work: E. g. bipolar degradation doesn't constitute a problem in today's SiC devices when operated in the range of nominal current, and their power cycling capability has been successfully optimised to reach a comparable level as conventional silicon devices, taking into account the different material properties. This has been reached with newly developed packages which often use sinter connections and partially permit double-sided cooling. Ongoing work e. g. refers to the methods for power cycling tests which need to cope with the known drift effects of SiC MOSFETs' threshold voltage.

Their short circuit capability would be desirable in many applications but increasing it by device design turns out to be costly. As an alternative, the devices may be monitored using e. g. dedicated driver circuits, allowing to turn short circuits off immediately and detect possible damages. While earlier mostly drivers for silicon MOSFETs have been used to control SiC and GaN transistors, the latters' increasing use has permitted the development of dedicated drivers. This is in particular promising for GaN HEMTs with their relatively low allowed gate voltage range; as the devices are lateral anyway, the integration of a driver circuit and also possibly of more circuit elements — like a complete phaseleg — constitutes a promising approach, which amongst others solves many issues related to inductive parasitics in conventional packages and circuit layouts.

This is directly related to the addressed aspect of circuit and system design: Electromagnetic compatibility plays an important role here and will be strongly influenced by oscillations triggered by the switching actions; recent methods to minimise these effects have been explained as well as the impact of voltage change rates on isolation systems. Obviously designers can use a variety of tools to investigate particular aspects, nevertheless their holistic knowledge and experience of how to properly design a circuit with wide bandgap devices is of great importance. As a further outlook, device and circuit optimisation for special requirements — like under high temperature conditions or exposure to cosmic ray — has been addressed. This may require measures concerning the semiconductor devices themselves as well as their packages. Probing even further, devices made of gallium oxide or diamond are under investigation.

Conclusion and Outlook

The findings as briefly summarised above illustrate the fast development of wide bandgap power semiconductors and their successful use in industry. This is beneficial for power electronics as a key technology in various areas, such as energy efficiency, usage of renewable sources for electric energy supply, e-mobility or also automation. Both, SiC and GaN devices are available in continuously increasing production volumes. They are widely applied in commercial products and allow to optimise those with respect to e. g. efficiency or miniaturisation. Nevertheless, research, development and also standardisation are ongoing to further exploit the possibilities of wide bandgap devices in power electronics. The European Center for Power Electronics (ECPE) is a stakeholder in this area, bringing together industrial partners and research institutions. After the broad interest of far more than 200 international participants this year, ECPE will anounce the next SiC & GaN User Forum in 2023. There will be the occasion to report the progress achieved since today — and to celebrate the jubilee of the 10th event within this successful series.

www.ecpe.org www.uni-magdeburg.de/llge

Compact Switcher Reduces Component Count

Power Integrations announced LinkSwitch™-TNZ, a switching power supply IC that combines offline power conversion, lossless zero-cross detection and, optionally, X-capacitor discharge functions in a compact SO-8C package. The LinkSwitch-TNZ IC can be used for non-isolated buck and buck-boost power supplies up to 575 mA output current and provides up to 12 W output for universal-input

isolated flyback designs. Adnaan Lokhandwala, product marketing manager at Power Integrations said: "The new LinkSwitch-TNZ ICs provide an accurate signal indicating that the sinusoidal AC line is at zero volts. This signal is used by smart home and building automation (HBA) products and appliances to control the switching of relays, IGBTs and TRIACs to minimize switching stress and system in-rush current. LinkSwitch-TNZ's detection of the zero-cross point consumes less than 5 mW, allowing systems to reduce standby power losses versus alternative approaches that require ten or more discrete components and burn 50 to 100 mW of continuous power."

LinkSwitch-TNZ ICs provide light-load efficiencies, enabling more system features to be powered while meeting stringent standby regulations such as: the European Commission (EC) standard for home appliances (1275), which requires equipment to consume no more than 0.5 W in standby or in off mode; ENERGY STAR's version 1.1 for Smart Home Energy Management Systems (SHEMS), which limits standby consumption of smart lighting control devices to 0.5 W; and China's GB24849, which limits the off-mode power consumption in microwave ovens to 0.5 W.

www.power.com

Miniature Buck Converter Delivers 4A

RECOM has added a 4A option to its RPX series of miniature buck converters. The RPX-4.0 is rated to 3.8 to 36V input and programmable 1 to 7V output at 4A. With a compact 5mm x 5.5mm footprint and low 4.1mm height in a thermally-enhanced QFN package, the buck module pushes the limit on power density. The product

features on-off control, a power good signal, and soft start, and is fully protected including under-voltage, short-circuit, over-current, and over-temperature. The RPX-4.0 efficiency is high, allowing full power operation up to 65°C and derated operation up to 90°C. Construction follows the RECOM '3D Power Packaging®' technology for high power density, with flip-chip on leadframe construction, an integrated shielded inductor for low EMI, and intelligent control of switching frequency to maintain high efficiency even at light load. The RPX-4.0 needs just voltage setting resistors and input/output capacitors for a complete high-performance solution and is delivered with the RECOM 3-year warranty. An evaluation board, RPX-4.0-EVM-1, is also available, allowing customers to exercise all of the product features and optimize filtering to meet target system requirements. "We are excited to launch the latest in our RPX series of buck converters" commented Matthew Dauterive DC/DC product manager of RECOM, "Users will find it particularly suitable for industrial automation, test and measurement, portable devices, and high density or weight-sensitive applications".

www.recom-power.com

80V Withstand 5A Output Power Supply ICs

ROHM announces the buck DC/DC converter ICs with built-in MOSFET, BD9G500EFJ-LA and BD9F500QUZ, that support high voltages and currents in factory automation equipment such as PLCs/inverters, and 5G base stations that handle high power. The BD9G500EFJ-LA and BD9F500QUZ are non-isolated DC/DC converter ICs developed by utilizing proprietary analog design technology based on high voltage BiCDMOS power processes to provide the power supply functionality required by increasingly sophisticated industrial equipment. In addition to a best-in-class 80V withstand voltage for 48V power supply systems, the BD9G500EFJ-LA with built-in MOSFET delivers the largest output current in its class (5A), contributing to higher reliability and functionality in charging and 5G base stations that handle large power. At the same time, the BD9F500QUZ with built-in Nano Pulse Control™ technology achieving a high step-down ratio provides 39V withstand voltage and 5A output current in a compact, low-profile package (3.0×3.0×0.4mm). Moreover, the product features an over current protection as SEL1/SEL2 pins can be selected. These features are ideal for 24V power supply systems – enabling support for higher functionality and greater

miniaturization in a wide range of advanced industrial equipment (i.e. factory automation).

www.rohm.com

Precision Current Sense Resistor

Bourns announced the availability of smaller package sizes and feature options in its Model CFN Metal Foil Current Sense Resistor Series. Miniature 0402 and 0603 packages were introduced to the Model CFN series as well as a lower TCR option of ±50 ppm/°C in the 0603 and larger package sizes. Using Bourns' metal foil technology construction enables the current sense resistors to provide low TCR, low inductance, low noise, excellent reliability and very low resistance values. These attributes make the Model CFN series an optimal current sensing solution for power supply, stepper motor drive, and input amplifier applications. The smaller sizes are particularly well-suited to meet the space-constrained requirements of mobile device designs.

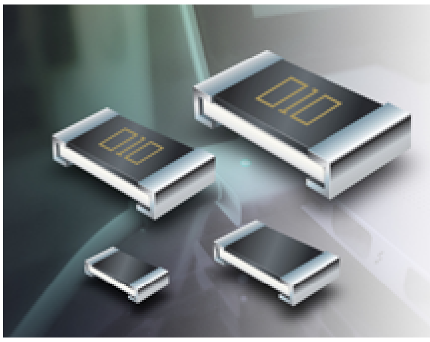

Ever important in current sensing is having a suitably low TCR, which is determined by characteristics such as the materials used in the resistive element, power rating, and physical size of the component. Bourns has leveraged metal foil technology to achieve lower resistance values, ranging from 5 to 40 milliohms, and still provide power ratings of 0.25 to 1 W in components small enough for mobile applications. Combining the new ±50 ppm/°C option with the low resistance values helps minimize self-heating so the resistor remains reliable and stays within its 1-5 percent tolerance over time.

www.bourns.com

Expanding Product Family with Latest 80 V and 200 V Offerings

EPC advances the performance capability while lowering the cost for off-the-shelf gallium nitride transistors with the introduction of EPC2065 and EPC2054.

The EPC2065 is an 80 V, 3.6 mΩ, 221 Apulsed eGaN FET in a 7.1 mm^2 chip-scale package. The small size and superior efficiency reduce overall power system size and weight and make it ideal for 32V-48V BLDC motor drive applications for eMobility ebike and escooters, service, delivery, logistic robots, and drones. In these applications the driver is integrated with the motor and miniaturization is a key factor. The ability to operate with significantly shorter dead times results in less noise and less EMI. The device is capable of high frequency operation to achieve the highest density for high frequency DC-DC converters for computing and industrial applications and for synchronous rectification.

The EPC2054 is a 200 V, 3.6 mΩ, eGaN FET in a tiny 1.69 mm^2 chip-scale package. The device can deliver 32 A pulsed current is an extremely small size, with very fast on-off transition times and super small capacitance and inductances, that make it ideal for industrial Lidar/ToF applications. The low resistance, low switching losses, no reverse recovery charge, fast switching, high frequency capability, and the tiny footprint make the EPC2054 a cost effective and high-density solution for a wide range of applications including, but not limited to, high frequency DC-DC, synchronous rectification, wireless power, class-D audio, Automation, Solar and Optical.

www.epc-co.com

Family in TO-247-3-HCC Housing Improves Isolation Voltage Rating

Infineon Technologies introduces the 650 V TRENCHSTOP™ 5 WR6 family in a discrete housing. The family comes in a TO-247-3-HCC package and offers a broad portfolio comprising 20 A, 30 A, 40 A, 50 A, 60 A and 70 A current ratings. The devices can easily be used for replacing previous technologies like Infineon's TRENCHSTOP 5 WR5 and HighSpeed 3 H3 as well as competitor technologies. The family is optimized for power factor correction (PFC) for residential and commercial air conditioning systems as well as welding applications. The TRENCHSTOP 5 WR6 switches provide very low conduction losses (30 A, 1,45 V at 25°C) as well as lowest switching losses (30 A, 1,55 mJ at 175°C). They feature a very low saturation voltage (V CE(sat)) of 1,45 V and a monolithically integrated diode with optimized forward voltage for the target applications.

This results in best-in-class performance while enabling a low BOM cost. Additionally, the device leverages the performance advantage of the TRENCHSTOP 5 WR5 series, the predecessor to the TRENCHSTOP 5 WR6 series.

The TO-247-3-HCC housing of the WR6 family increases the creepage and clearance distances thus improving the isolation voltage rating. With this, the product family enables more reliable system designs that are resistant against contamination and condensation which e.g. often occur at AC outdoor units. The TRENCHSTOP 5 WR6 reduces the total cost of ownership with less failure rate while it also enables higher switching frequency in application.

www.infineon.com

Point of Load Converters Target USB-PD Applications

Silanna Semiconductor focuses on power management challenges with devices that combine best-in-class power density and efficiency performance with unprecedented BoM savings. Operating at a switching speed of 667kHz, the SZDL3105B fully-integrated DC/DC converter (buck regulator) can supply up to 5 amps and 100 watts of output power. It accommodates industry-leading wide input and output ranges that support up to 27VDC input and is supplied in a tiny 4mm x 4mm QFN package.

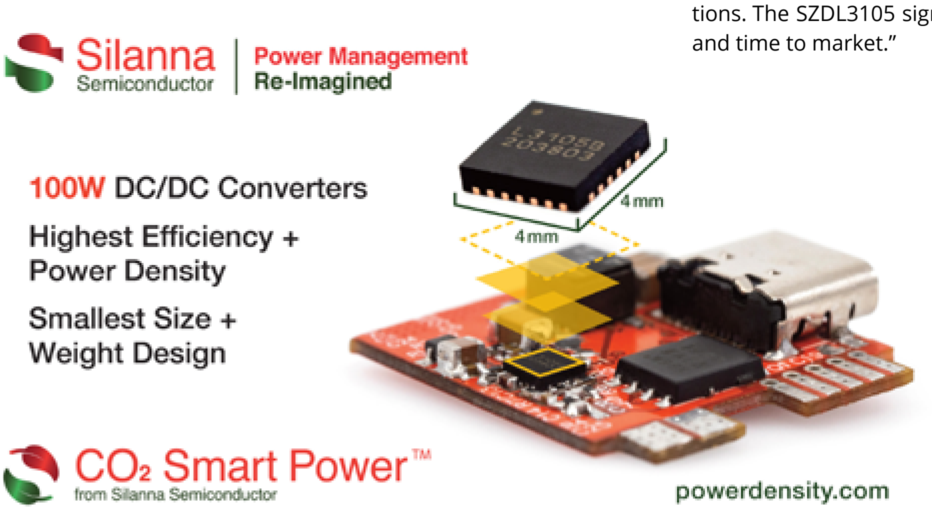

Tim Wilhelm, Director of Marketing, explained, "Higher switching frequency means a smaller, lower cost, higher performing output filter that has delighted the clients we have sampled. The SZDPL3105B device enables ground-breaking efficiencies in the smallest size and weight designs. Our support tools give customers the flexibility and confidence to quickly increase the performance efficiency. This ultimately increases power density with volumes approaching 12% of that required by low-frequency competitive solutions. The SZDL3105 significantly reduces BOM cost, design cycles and time to market."

The SZDL3105B has features that optimize its performance in USB port power supply applications. Extremely low operating power dissipation enables the very low no-load power that is an important specification for regulatory certification. Internal and external feedback resistor divider flexibility supports custom design, while a momentary internal feedback path allows for clean and well-controlled start-up operation until external USB port controllers can bias themselves and smoothly take over control of the output voltage.

www.powerdensity.com

Coating Method Aerosol Deposition Available for Industrial Use

Heraeus broadens the application range of the Aerosol Deposition coating method. So far, the technology, which was developed in Japan, has been used mainly in Asia for coating of components for plasma etch chambers. Although the coating method offers many advantages, other industries have hardly applied it until now. "However, feasibility studies by universities such as the University of Bayreuth have shown that Aerosol Deposition offers advantages also for other applications," Dr. Ilka Luck says, Head of Heraeus High Performance Coatings. She sees potential in sensor technology, power electronics, battery, and medical technology, among others.
"We have worked intensively over the past two years on optimizing processes and machines for production on industrial scale. As a result, we are the only supplier that accompanies customers all the way from feasibility study to series production," Luck comments. The technology is particularly promising when conventional methods do not achieve the required quality, or the desired coating cannot yet be produced at all.
Aerosol Deposition is a process for producing thin material layers. Material particles are accelerated to a speed of several hundred meters per second with the aid of a carrier gas. These then hit a surface, the so-called substrate, where they form a closed film.

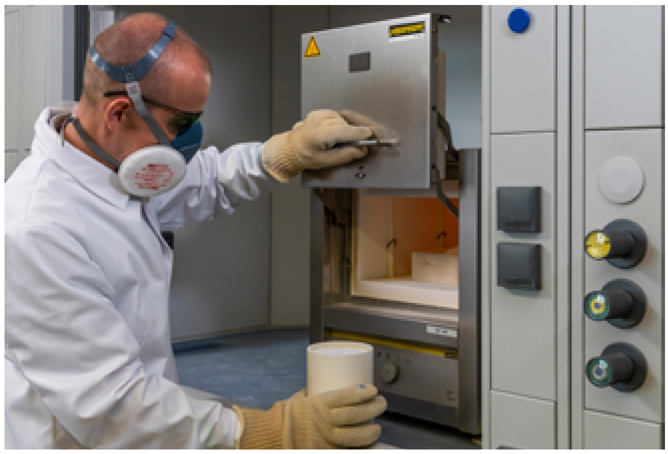

Aerosol Deposition has no fundamental limitations in terms of coating materials or substrates that can be used. "We already use both for coating, metals and ceramics. The only requirement for its use is that the material is available as a processable powder," Luck explains.

www.heraeus.com

Advertising Index